Thus α-tocopherolhydroquinone, derived from (2*R*,4′*R*,8′*R*)-α-tocopherol,[2a] regenerates the same tocopherol, with 100% retention of configuration, upon cyclization with *p*-toluenesulfonic acid in refluxing benzene.[8]

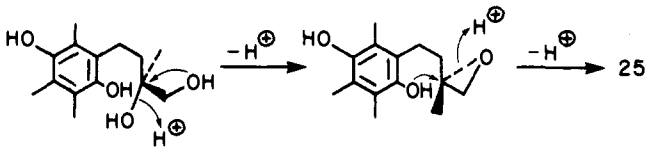

28 35

(30) We are grateful to a referee for suggesting an attractive, related mechanistic rationale for the clean retention of configuration observed in the conversions of **22** and **28** to **25**. This involves the intermediacy of quinone ketal **24** formed in small quantity from **28** by air oxidation (via **27**). Reduction of **24** by hydroquinone **28** then produces **25** and regenerates **27**, thus establishing a catalytic redox cycle. In this regard, it should be noted that, because of their extreme air sensitivity, hydroquinones **22** and **28** contained trace quantities of the corresponding quinones the formation of which could not be avoided.

(31) Ratcliffe, R.; Rodehorst, R. *J. Org. Chem.* **1970**, *35*, 4000–4002.

(32) This aldehyde was first prepared by Dr. K.-K. Chan of our laboratories, starting from the *S* acid **23**,[8] by a sequence involving formation of the methyl ester (methyl iodide, $NaHCO_3$, DMF, room temperature), benzylation of the 6-hydroxyl function (benzyl chloride, K_2CO_3, DMF, room temperature), and partial reduction (diisobutylaluminum hydride, −70 °C, hexane).

(33) The purified potassium ferricyanide oxidation product of natural (2*R*,4′*R*,8′*R*)-α-tocopherol is reported to exhibit $[\alpha]^{25}_D$ +31.5° (*c* 5, isooctane): Rubel, T. "Vitamin E Manufacture", Noyes Development Corp.: Park Ridge, N.J., 1969; pp 95–99.

Syntheses and NMR Characterization of Chelated Heme Models of Hemoproteins[1,2]

T. G. Traylor,* C. K. Chang, J. Geibel, A. Berzinis, T. Mincey, and J. Cannon

Contribution from the Department of Chemistry, D-006, University of California, San Diego, La Jolla, California 92093. *Received June 27, 1977*

Abstract: Convenient syntheses of "chelated heme" compounds from naturally occurring hemes are described. NMR studies of the carbon monoxide complex of chelated protoheme serve to characterize this model compound in solution. Chelated protoheme, having a "proximal" imidazole covalently attached, displays spectra and kinetics and equilibria of reaction with dioxygen and carbon monoxide that are similar to those of R-state hemoglobin, making chelated protoheme unique among model compounds.

Hemoproteins that transport dioxygen have dioxygen binding sites which consist of a protoheme molecule held in a globular protein by an imidazole-iron bond and by other noncovalent bonding.[3] Although not attached by covalent bonds as is the cytochrome *c* heme, the protoheme in hemoproteins such as hemoglobin or myoglobin is bound so strongly as to make the hemoprotein behave as a single molecule. Furthermore, the Fe(II) is five-coordinated in the deoxy form of these hemoproteins. The function of these hemoproteins is simply the reversible binding of triplet dioxygen without themselves undergoing oxidation to Fe(III):

$$\mathrm{Fe(II)} + \mathrm{O_2} \underset{5\text{ to }2500\ \mathrm{s^{-1}}}{\overset{10^6\text{-}10^8\ \mathrm{L\ M^{-1}\ s^{-1}}}{\rightleftharpoons}} \mathrm{Fe^{II}O_2} \nrightarrow \mathrm{Fe(III)} \qquad (1)$$

Because respiration is controlled by the variations in the rate constants shown in eq 1, it is of great interest to determine the sources of these variations.[3,4] The obvious way to find out what affects the kinetics and equilibria of dioxygen binding is to prepare small model compounds that reversibly bind dioxygen and to vary the structures and environment in the study of these compounds.[5-7] However, when hemin compounds and imidazoles were mixed in a solvent, reduced to Fe(II), and treated with oxygen, two things happened to prevent such mixtures from mimicking hemoglobin behavior. First, two imidazoles are bound, converting the heme to a hexacoordinated hemochrome unlike the five-coordinated heme in hemoglobin.[3] Secondly, such mixtures were thought to oxidize the Fe(II) too fast to allow reversible oxygenation to be studied,[8] an opinion which no longer holds.[5b]

The oxidation of hemes to hemins in solution is much more rapid than are the corresponding oxidations of myoglobin or hemoglobin. One mechanism of such oxidation was proposed by Cohen and Caughey,[9] based upon the observation that heme oxidation in solutions containing pyridine is second order in the heme and first order in dioxygen:

$$\mathrm{Fe(II)} + \mathrm{O_2} \rightleftharpoons \mathrm{Fe^{II}\text{-}OO} \qquad (2)$$

$$\mathrm{Fe^{II}\text{—}OO} + \mathrm{Fe(II)} \rightarrow \mathrm{Fe^{II}\text{-}OO\text{-}Fe^{II}} \qquad (3)$$

$$\mathrm{Fe\text{-}OO\text{-}Fe} \rightarrow\rightarrow \mathrm{Fe(III)} + \mathrm{H_2O} \qquad (4)$$

This mechanism has been further documented by the observation that at high oxygen pressure (0.1 to 1 atm) and strong dioxygen binding, the rate is second order in Fe(II) and *inverse* first order in dioxygen,[10] as required by eq 3. Evidence for the existence of an Fe-OO-Fe structure at low temperature has also been presented.[11]

We have presented two methods of studying reversible oxygenation of simple heme compounds. First, oxidation is not as fast as had been presumed, and rapid kinetic and spectroscopic methods can be applied to reversible oxygenation of almost any heme model system.[12a,b] Secondly, carbon monoxide can be used to protect against oxidation and removed quickly by flash photolysis, allowing the rapid spectroscopic and kinetic methods to be used in mixtures of CO and O_2.[12b,c] Because the heme-oxygen complex is formed and dissociated faster than is the heme-carbon monoxide complex, exactly as with hemoproteins, the flash photolysis method is applicable to simple model compounds[12b,c] (Hm = heme, B = proximal base) (eq 5).

$$\mathrm{BHmCO} \underset{l' = 10^5\text{-}10^8\ \mathrm{M^{-1}\ s^{-1}}}{\overset{h\nu \quad l = 0.01\text{-}1000\ \mathrm{s^{-1}}}{\rightleftharpoons}} \mathrm{BHm} \underset{k = 5\text{-}1000\ \mathrm{s^{-1}}}{\overset{k' = 10^7\text{-}10^9\ \mathrm{M^{-1}\ s^{-1}}}{\rightleftharpoons}} \mathrm{BHmO_2} \qquad (5)$$

The second problem of maintaining a single species, five-coordinated heme behavior as do hemoproteins was solved by preparing chelated hemes in which five-coordination is

0002-7863/79/1501-6716$01.00/0

maintained by having the "proximal" imidazole covalently attached (see Figure 1). This is, to date, the only convenient method allowing dynamic hemoprotein model studies in solution to be made.

In this paper we present the details of syntheses of chelated hemes, completely characterize one of these systems in solution by NMR, and describe the spectroscopic and kinetic properties of chelated hemes and their dioxygen and carbon monoxide complexes.

Results

Syntheses. Our approach toward the syntheses of hemoprotein "active-site sections" is based upon the covalent attachment of side chains having the requisite base to constitute the proximal or distal base and proper chain length for iron chelation in the hemoprotein. This was accomplished by coupling various pyridine, imidazole, or other derivatives to the heme through the propionic acid side chains as had been done by Lautsch et al.,[13] Losse and Müller,[14] Warme and Hager,[15] and by van der Heijden et al.[16] While in this earlier work

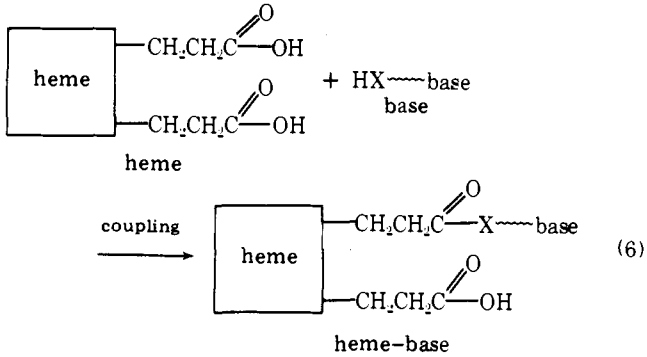

(6)

naturally occurring peptides or amino acids were used for this coupling, we preferred to use synthetic bases designed to achieve certain desired geometry, proximal base structure, or porphyrin ring structure. The carbonyl attachment was made through either an ester or an amide function, and the usual coupling procedures that have been developed for peptide syntheses should be applicable. However, these procedures are usually designed to waste the acid portion of the coupling mixture and consequently often lead to undesired porphyrin derivatives that are difficult to remove. We therefore explored a wide variety of coupling methods. In one approach, the porphyrin dimethyl ester was partially hydrolyzed and, after purification, the monoacid was coupled to a primary amine or alcohol containing the desired proximal base (P ≡ porphyrin ring) by the pivalyl chloride method.[17,18]

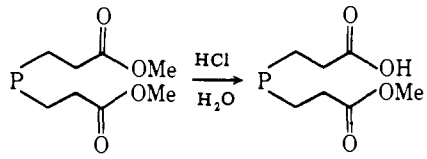

(7)

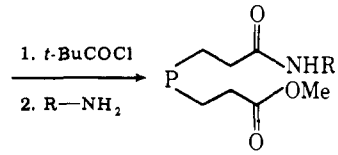

(8)

An alternative procedure that is effective for most simple primary amines such as 1-[3-aminopropyl]imidazole employs commercial protoheme directly in a one-pot reaction to produce, alternately, the diamide, the monoamide-monoacid, or the monoamide-monoester, depending upon amounts of amine added and upon workup procedures employed. Treatment of protohemin with a slight excess of pivalyl chloride in pyridine followed by addition of only enough amine to react with one

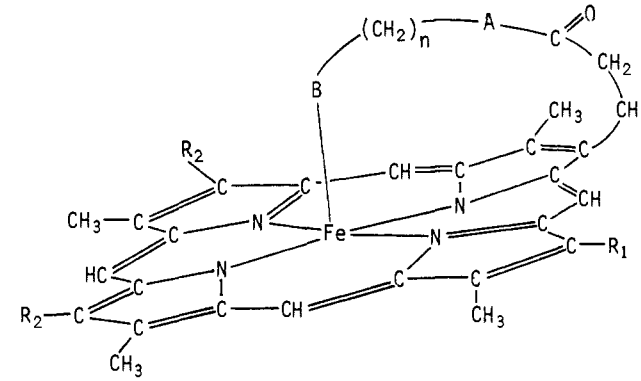

Figure 1. Chelated hemes.

of the two anhydride groups and quenching with methanol produced, after chromatography, about 30% yield of protohemin monomethyl ester monoamide derivative (Hm^+ = protohemin chloride ring).

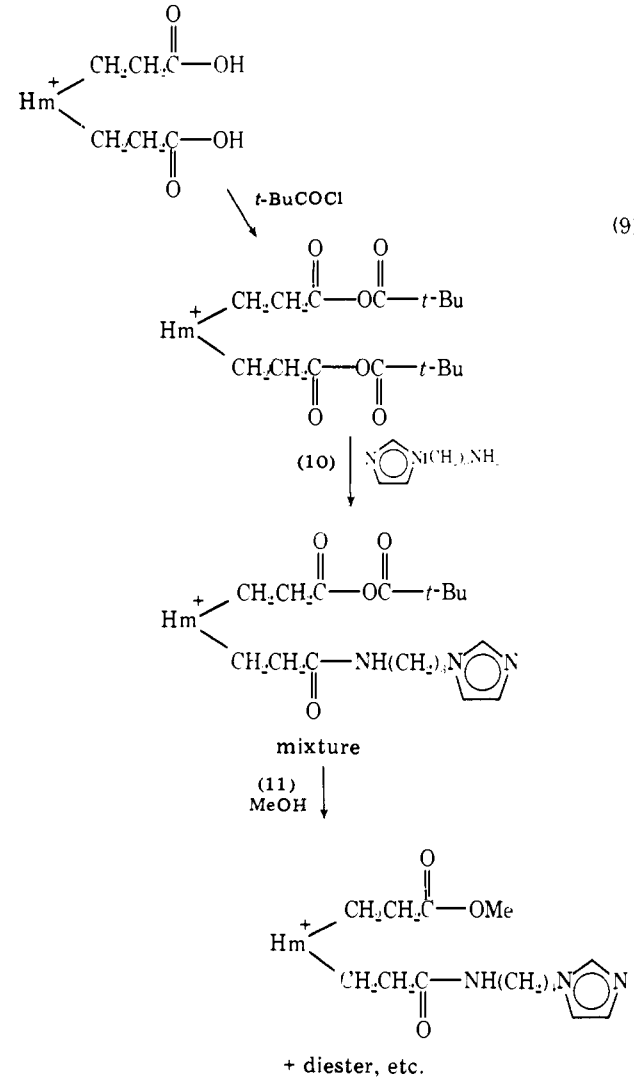

(9)

Alternatively, the reaction mixture can be quenched with water to produce the monoacid (eq 12). These methods depend upon the easy chromatographic separation of the diacid, monoacid, diester, and mono- and diamides.

The chelated hemin chloride compounds, after purification by column chromatography to the point where one-spot thin-layer chromatography was observed with several solvents, gave satisfactory analyses and NMR spectra. Because our syntheses

Table I. Structures of Heme Compounds[a,b]

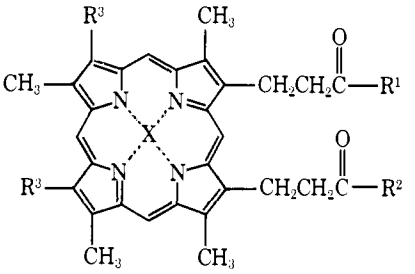

compd (named as the Fe(II) derivative)	R^1	R^2	R^3
1, chelated pyrroheme	$-NH(CH_2)_3N$⬡N	*c*	Et
2, mesoheme diacid	$-OH$	$-OH$	Et
3, mesoheme dimethyl ester	$-OCH_3$	$-OCH_3$	Et
4, mesoheme monoacid	$-OH$	$-OCH_3$	Et
5, chelated mesoheme	$-NH(CH_2)_3N$⬡N	$-OCH_3$	Et
6, dichelated mesoheme	$-NH(CH_2)_3N$⬡N	$-NH(CH_2)_3N$⬡N	Et
7, chelated mesoheme acid	$-NH(CH_2)_3N$⬡N	$-OH$	Et
8, pyridine chelated mesoheme	$-O(CH_2)_3$-⬡N	$-OCH_3$	Et
9, chelated protoheme	$-NH(CH_2)_3N$⬡N	$-OCH_3$	$-CH=CH_2$
10, dichelated protoheme	$-NH(CH_2)_3N$⬡N	$-NH(CH_2)_3N$⬡N	$-CH=CH_2$

[a] The numbers **1**, **2**, etc. refer to the Fe(II) or heme compound shown. The corresponding porphyrins, having Fe(II) replaced by two H^+ ions, are indicated by adding P to the number, etc. Thus, e.g., **2** = mesoheme, **2P** = mesoporphyrin, $\mathbf{2}^+Cl^-$ = mesohemin chloride, **2**-CO = carbon monoxide complex of mesoheme. [b] As a result of the method of synthesis, each of these compounds consists of a 1:1 mixture of the compound shown and that having R^1 and R^2 interchanged. See the NMR results. [c] In compound **1**, the heme is pyrroheme, in which the entire group $-CH_2CH_2CO_2R$ is replaced by $-H$.

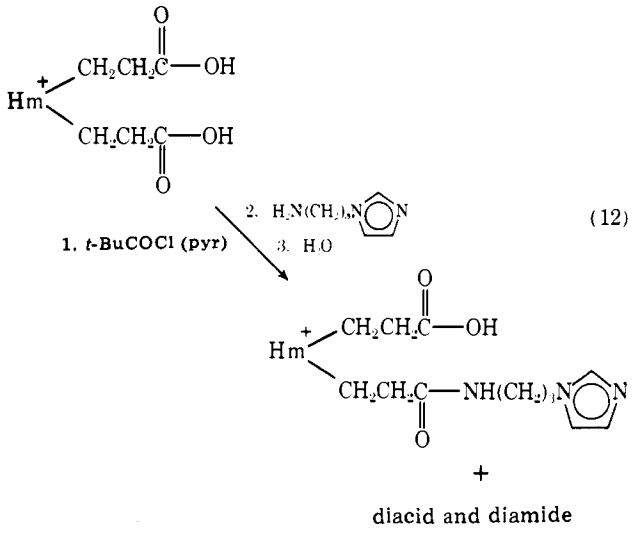

(12)

consist of simple derivatizations of well-known compounds, the structure proofs are rather straightforward. UV-visible spectra are, in these cases, indications of structure. The coupling of hemin rather than porphyrin derivatives avoids the difficulties of adventitious photooxidation often observed with porphyrin derivatives.

The compounds discussed in this paper are shown in Table I.

NMR Studies of Heme Complexes. The 220-MHz proton NMR spectrum of the ferrous CO complex (**9**-CO) is shown in Figure 2. The shifts of the porphyrin substituents are consistent with those previously published for low-spin ferrous complexes. At the concentrations studied (0.02–0.05 M), **9**-CO and the other low-spin ferrous complexes were free of the concentration-dependent resonance shifting that is often important in porphyrin NMR.[19,20] Assignment of the meso and vinyl protons was made by analogy to the assignment of protoporphyrin IX dimethyl ester.[21] The bound imidazole shifts are similar to those reported for an imidazole complex of ruthenium carbonyl mesoporphyrin IX dimethyl ester.[22] The assignments for chelated protoheme-CO (**9**-CO) and dichelated protoheme (**10**-CO) are shown in Figure 3, and those for an analogous heme-imidazole-CO mixture (**11**-CO) are shown in Figure 4.

Visible spectra obtained in the NMR tube before and after the NMR experiment on **9**-CO are shown in Figure 5. The Fe(III) form ($\mathbf{9}^+$ Cl), in Me_2SO-d_6 shows a broad visible band around 570 nm and very broad lines in the NMR. Reduction with aqueous dithionite under Ar leads to visible absorptions at 525 and 555 nm, indicative of the ferrous Me_2SO–imidazole complex. The corresponding NMR spectrum shows the imidazole to be bound, but the side-chain resonances are substantially broadened. Addition of 1 mL of CO (excess) to the sample results in visible absorptions at 564 and 536 nm and the NMR spectrum in Figure 2. Identical peak positions and relative intensities are obtained for visible spectra at dilute (micromolar) concentrations in Me_2SO. The λ_{max} obtained for CO complex **9**-CO also compares well to those obtained in cetyltrimethylammonium bromide ($CetMe_3NBr$) buffer and other solvents. (Compare the spectrum in Figure 5 with that in Figures 9 and 10 in the spectroscopy section below.)

Similar experiments were carried out with dichelated protoheme (**10**-CO), in which both propionic acid groups of protohemin are derivatized as imidazolyl side chains. The visible spectrum of **10**-CO is identical with that of the monochelated heme (**9**-CO). The NMR spectrum is also identical, except for peaks identified with the additional unbound side chain (see Figure 3). As will be shown below, complex **10**-CO was quite useful in making structural assignments.

For purposes of comparison, the NMR spectra of a number of ferrous CO complexes were measured, using protoheme IX dimethyl ester and an externally added alkylimidazole as the base. As before, the visible spectrum of the NMR sample could be measured without removing the sample from the tube. This allowed preparation of a Me_2SO–heme-CO complex, followed by titration with a ligand while following the change in ligation by the usual method of visible spectroscopy. The binding of simple alkyl imidazoles to a five-coordinated CO complex is strong enough to completely displace Me_2SO, but the sterically hindered 2-methylimidazoles require addition of a several-fold excess of base to obtain acceptable amounts of bound imidazole.[23] The faster off-rates of the 2-methylimidazole also result in some broadening of the bound resonances.[24]

The chemical shifts of alkylimidazoles bound as ferrous CO complexes are listed in Table II. They are of two groups, R^2 being either $-H$ or $-CH_3$. As expected, substituents at the 2 or 4 positions of the imidazole are most strongly shifted upfield by the ring current of the macrocycle, which increases in strength both approaching the porphyrin plane and the ligand axis through the metal.[25] Thus, protons at the 2 or 4 positions are shifted ~7 ppm upfield upon binding, and 2-methyl groups are shifted ~4.4 ppm. The resonances for the 4 protons are

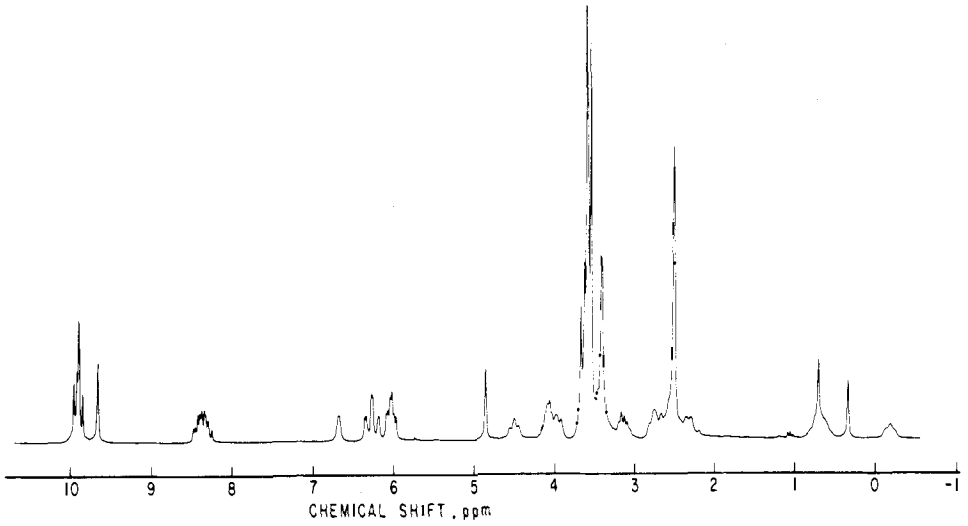

Figure 2. 220-MHz NMR spectrum of chelated protoheme **9**-CO, 0.03 M in Me_2SO-d_6, under 1 atm of CO. The large peak at δ 2.5 is due to solvent.

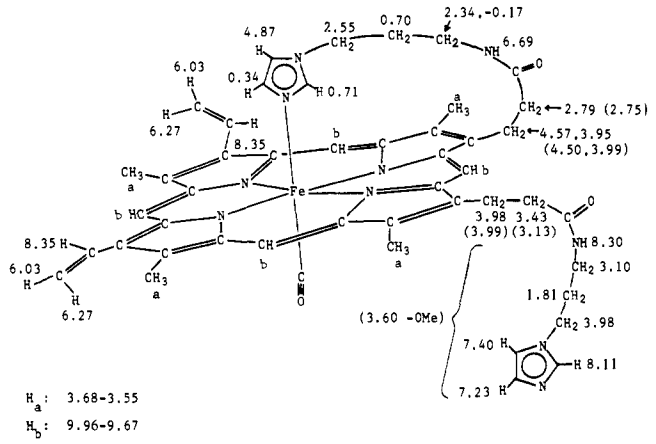

Figure 3. Chemical shifts of the dichelated protoheme **10**-CO and chelated protoheme **9**-CO in Me_2SO-d_6. Values in parentheses refer to **9**-CO for those shifts that were measurably different from **10**-CO.

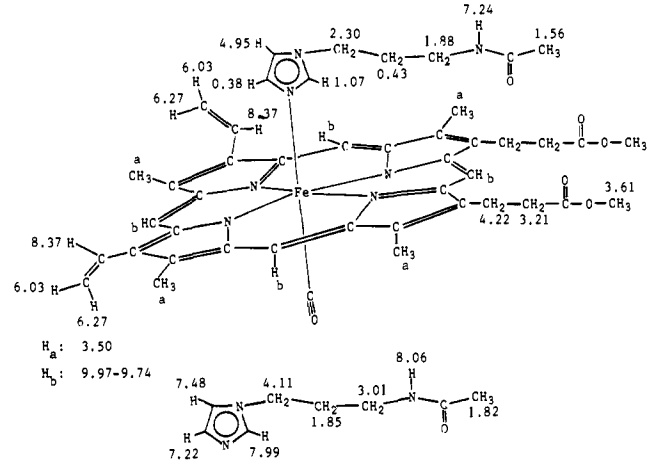

Figure 4. Chemical shifts of the protoheme IX dimethyl ester-CO-[1-(3-acetamidopropyl)imidazole] complex (**11**-CO) in Me_2SO-d_6.

shifted 0.64–0.67 ppm and those of the 5 protons 0.06–0.16 ppm upfield compared to those of the unhindered *N*-alkylimidazoles. We attribute this to the tilting of the imidazole ring in the direction to bring the 4-H nearer the porphyrin plane, due to the bulk of the 2-CH_3 group. This tilting has been demonstrated by X-ray crystallographic studies of low-spin Co(II) 2-methylimidazole complexes[26] and was postulated to explain differential shifts in Fe(III) porphyrin complexes.[27]

The data from the external base complexes of Table II made assignment of the imidazole resonances of chelated protoheme (**9**-CO) straightforward. Assignments of the side-chain resonances were not as obvious. The multiplets at 4.57 and −0.17 ppm had areas of only 1 proton, another multiplet was masked by the imidazole singlet at 0.7 ppm, and the large Me_2SO solvent peak occurred among a number of resonances, making integration impossible.

The assignments were finally verified by use of saturation-transfer techniques.[28] The exchange rate of 1-methylimidazole, bound as a ferrous CO complex, with free 1-methylimidazole is on the order of 0.5 s^{-1},[29] which is competitive with the T_1 relaxation of the bound resonances. Thus, using a complex of 1-methylimidazole with ferrous CO and ~50% excess of base, saturation of the free methyl resonance results in a decrease in intensity of the bound methyl resonance. A similar result is obtained for the imidazole C-H resonances. The amount of saturation transfer observed depends on the relative popula-

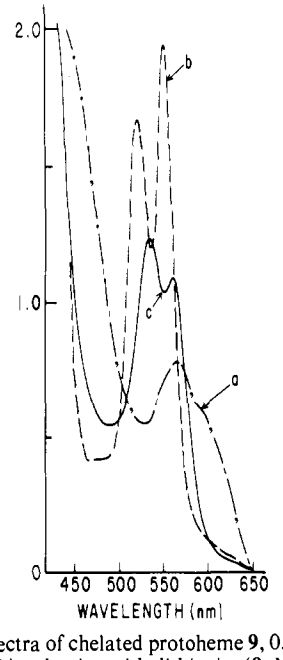

Figure 5. Visible spectra of chelated protoheme **9**, 0.03 M in Me_2SO-d_6: (a) hemin (**9**$^+$Cl); (b) reduction with dithionite (**9**-Me_2SO); (c) addition of 1 atm of CO (**9**-CO).

Table II. Chemical Shifts of Alkylimidazoles in Ferrous CO Complexes of Protoheme IX Dimethyl Ester, 0.03 M in Me_2SO-d_6 in Parts per Million Downfield of Tetramethylsilane

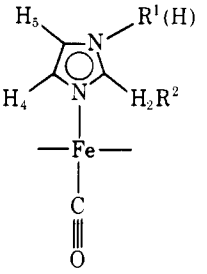

substit position			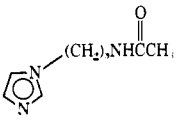		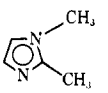	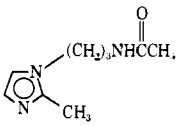
1	*a*	1.99	2.30	*a*	1.99	
2	1.00	1.05	1.07	−2.09	−2.15	−2.19
4	0.42	0.36	0.38	−0.22	−0.30	−0.29
5	4.88	4.86	4.95	4.72	4.80	4.79

[a] No signal due to rapid exchange with solvent.

Table III. NMR Chemical Shifts of Side-Chain Protons in the Bound and Unbound Side Chains of Dichelated Protoheme (**10**) (see Figure 3) and the Protoheme Dimethyl Ester Complex with 1-[3-Acetamidopropyl]imidazole (**11**) (Figure 4) in Me_2SO-d_6

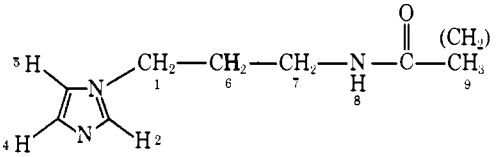

	shifts (δ) in bound side-chain CO complexes		shifts (δ) in unbound side-chain CO complexes		upfield shift (Δδ) upon binding $\delta_{unbound} - \delta_{bound}$	
	10-CO	**11**-CO	**10**-CO	**11**-CO	**10**-CO	**11**-CO
1	2.55	2.30	3.98	4.11	1.43	1.81
2	0.71	1.07	8.11	7.99	7.40	6.92
4	0.34	0.38	7.23	7.22	6.89	6.84
5	4.87	4.95	7.40	7.48	2.53	2.53
6	0.70	0.43	1.81	1.85	1.11	1.42
7	2.34, −0.17	1.88	3.10	3.01	0.76, 3.27	1.13
8	6.69	7.24	8.30	8.06	1.61	0.82
9	2.79	1.56	3.43	1.82	0.64	0.26

ıions of the bound and free sites and the relationships of the T_1's and exchange rates.[28] This technique was used in assignment of the previously mentioned ruthenium complex.[22]

The saturation transfer method is ideally suited to the covalently bound imidazole in **10**-CO in which equal populations of bound and free sites are available. The shifts of the unbound side chain are listed in Table III. By noting saturation transfers caused by irradiation of the known unbound side-chain resonances, the correct assignment can be seen directly. As there are large differences in chemical shift between bound and free sites, the entire side chain could be assigned this way. The resulting assignments are listed in Figure 3.

These results indicated the resonances of the methylene α ıo the bound imidazole are mostly obscured by the Me_2SO peak. To get around this problem we exploited the differences in T_1 of solvent and the side-chain resonances. T_1 measurements by inversion recovery[30] showed solvent to relax ~20 times slower than the propylamide side chain. Under these conditions, the solvent protons can be saturated with negligible effect on the side-chain resonances.[31] Thus, irradiation of the Me_2SO peak with just enough power to cause saturation results in the spectrum in Figure 6, which shows the resonances around 2.5 ppm. The methylene in question is now seen as a broad resonance at 2.55 ppm, between the previously assigned shifts at 2.79 and 2.34 ppm. Integration of this area indicates exactly five protons as required by the assignment.

Several interesting aspects of the spectrum can be noted. The methylene next to the amide nitrogen is dramatically split into shifts at 2.34 and −0.17 ppm, with geminal coupling $^3J_{HH}$ = 14 Hz. Similarly, the first methylene of the propionic amide is split into resonances at 4.57 and 3.95 ppm, $^3J_{HH}$ = 14 Hz.

Having established the assignment, what can we learn about ıhe details of the ligand binding? We should first like to demonstrate that the imidazole side chain is indeed internally bound as depicted in Figure 3. We would also like some information on the conformation of the side chain and what effect, if any, this has on imidazole and CO binding.

To these ends the NMR of the protoheme dimethyl ester complex (**11**-CO) was investigated. The external base is the acetamide of the same 3-(1-imidazolyl)propylamine used to synthesize the chelated model compounds. Using an excess of ligand, the chemical shifts of the bound and free sites can be obtained from the same solution as was done with **10**-CO. As before, visible spectra and saturation-transfer techniques were used to characterize **11**-CO. The resulting shifts are given in

Table III and Figure 4. From these data, the upfield shift, $\Delta\delta$, in parts per million for each position can be computed. This is the ring current-induced shielding or deshielding, which occurs when the ligand is brought from the "free" position in solution to the bound position on the iron. Inspection of the $\Delta\delta$ values for complex **11**-CO shows that proceeding out the side chain (positions 6–9) there is a steady decrease in $\Delta\delta$ values, to be expected on moving the protons away from the symmetry axis and (most likely) out into solution as well.

We now compare these to the $\Delta\delta$ values for the side chain of the chelated **10**-CO. Positions 1 and 6 are seen to have *smaller* $\Delta\delta$ values than the external base. One 7-H is shifted upfield only slightly, while the other experiences a greater $\Delta\delta$ than the 5-H of the imidazole! The 9-CH_2 of **10**-CO is shown as having an upfield shift. As it lies in the deshielding region of the ring current,[19] the effect amounts to *less deshielding* compared to the free side chain.

The following is an interpretation we feel is consistent with the above results. First, the chelating imidazole is complexed completely to the heme in **9**-CO. Any uncomplexed imidazole would have displayed resonances at δ 7.4, 7.23, and 8.11 as seen in **10**-CO. The decreased upfield shifts of positions 1 and 6 in **10**-CO are due to loss of free rotation in the chelated compound, i.e., the methylenes are constrained to point away from the porphyrin plane. The wide differences between the 7-H positions strongly suggest a conformation in which one CH is directed toward the macrocycle and the other away. The amide NH appears to lie closer to the porphyrin ring than in the external base. Less deshielding at the 9 position indicates a position above the porphyrin plane. The *increased deshielding* of one CH of the methylene α to the porphyrin to 4.57 suggests constraint of the CH to lie more in the plane of the porphyrin.

The pattern of $\Delta\delta$s clearly demonstrates that the side chain is folded over the heme, not only internally bound but in a relatively fixed conformation. If the compounds were forming dimers or polymers[32] by binding a noncovalently linked side chain, the ligand shifts would more closely resemble the external base complex **11**-CO and show resonances near δ 1.88, which we did not see. NMR of a chlorophyll model containing the same chelated imidazolyl side chain[33] shows the same pattern of bound resonances and upfield shifts.

We now turn to the position of the bound imidazole. Construction of a Corey–Pauling–Koltun (CPK) space-filling model shows the most suitable conformation of the side chain places the plane of the imidazole somewhat off the fourfold axes through the porphyrin nitrogens. This also relieves interactions of the 2,4 protons of the imidazole with these nitrogens. The desirability of such a structure has been demonstrated by X-ray analysis of various ligand–heme combinations.[34]

We have already shown the shift positions of the bound imidazole are sensitive to changes in the Fe–N bond angle. Comparison of $\Delta\delta$ values in Table III shows the 4 and 5 positions of the chelated imidazole to be the same as the external, unhindered base, but the 2 position is 0.48 ppm further upfield in the chelated model. This might seem to indicate a tilting of the imidazole toward the side chain; however, placement of the 2-H closer to the ring by tilting would necessitate an equal *uplifting* of the opposite 4-H, leading to a *smaller* $\Delta\delta$. Such an effect is not observed. It is also unlikely, in a six-coordinated low-spin CO complex, that the Fe will move out of plane and so cause anomalous shifts. Inspection of the CPK model shows the 2-H to lie close to the amide carbonyl, perhaps within the shielding anisotropy of the C=O bond. The upfield shift of 0.5 ppm experienced by this proton may easily be explained by such an interaction.

The NMR spectra of chelated hemes bearing ethyl or acetyl groups in place of vinyls show the 2-H to be shifted upfield by

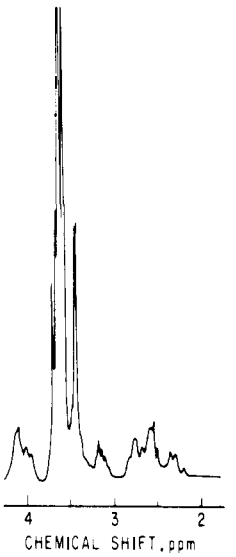

Figure 6. 220-MHz NMR spectrum of **9**-CO in Me_2SO-d_6 with saturation of the solvent peak.

the same amounts, relative to 1-methylimidazole. This occurs despite the varying intensities of ring current induced shifts caused by addition of electron-donating or -withdrawing groups to the heme and lends further support to this shielding phenomenon being due to the side chain, and not tilting of the imidazole–Fe bond.[35a]

We therefore conclude the imidazole position of **9**-CO is sterically unhindered. This is borne out by kinetics measurements, which show that the chelated hemes **5**-CO and a similar compound, having four rather than three (CH_2) groups between the two nitrogens, behave identically.[36]

While the shift positions of the substituents on the porphyrin periphery are as expected, some important changes in multiplicities are brought about by addition of the chelated side chain. External bases should be free to rotate among several equivalent positions relative to the porphyrin macrocycle; indeed, this randomness has presented a problem to crystallographic analysis of such complexes.[34] The chelated compound **9**-CO holds the imidazole in a unique position across the macrocycle. Since the natural heme is unsymmetrically substituted, and the coupling procedure should not discriminate between the two propionic acids, one would expect an equal mixture of isomeric complexes of **9**-CO (and of **10**-CO as well) depending on which propionic acid is derivatized (or which imidazole is bound in **10**-CO).

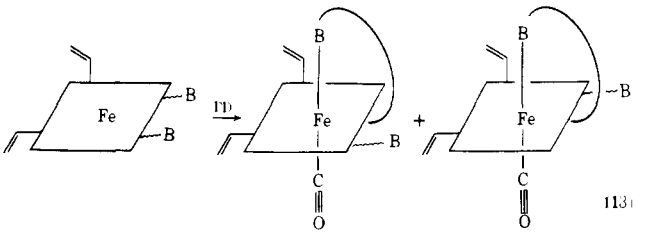

A comparison of the downfield regions of **9**-CO and **11**-CO is shown in Figure 7. In that of **11**-CO the meso protons appear as singlets and the vinyl methylenes as doublets. In the spectrum of **9**-CO (and in **10**-CO), we now see that two of the meso positions are split into doublets, and the vinyl methylenes now appear as triplets. As the meso protons are not coupled to any other protons, the apparent splitting is due to a mixture of nonequivalent isomers. In **11**-CO the vinyl methylenes appear as doublets due to fortuitous superposition of resonances from the 2 and 4 positions. This chemical-shift equivalence holds true for most external base complexes of ferrous protoheme

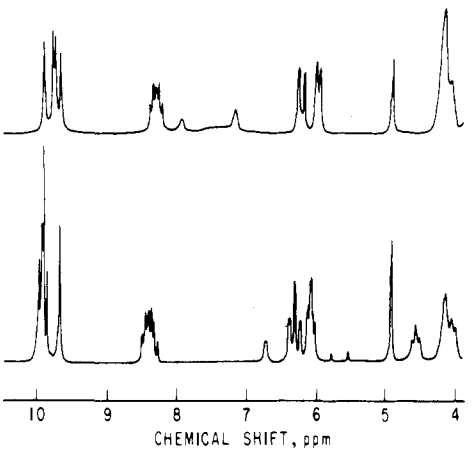

Figure 7. 220-MHz NMR spectra of **11**-CO (upper spectrum) and **9**-CO (lower spectrum) in Me_2SO-d_6. Peaks at δ 7–8 are due to excess alkylimidazole.

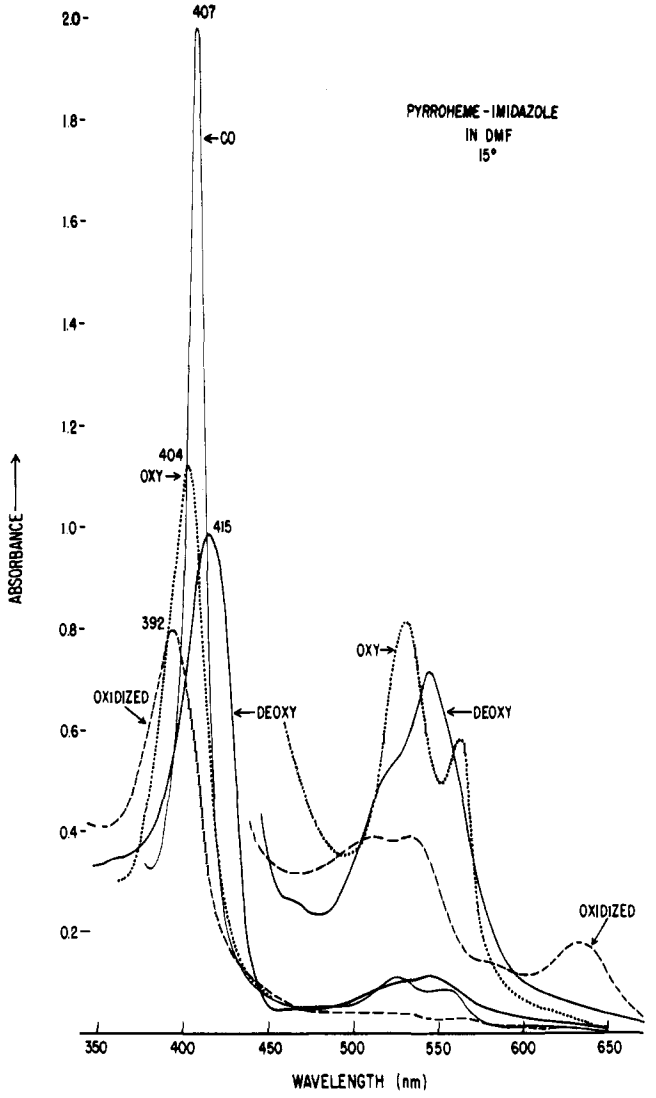

Figure 8. Spectra of chelated pyrroheme **1** in dry dimethylformamide at 15 °C as the hemin ($\mathbf{1}^+Cl^-$): (---) after reduction with Pd on charcoal as the heme (**1**) (—); after addition of 1 atm of O_2 gas (**1**-O_2) (···); after flushing the gas phase briefly with CO (**1**-CO) (—). Insets are on an expanded (×10) absorbance scale.

dimethyl ester (unpublished results). In **9**-CO the mixture of conformationally different isomers results in chemical nonequivalence between respective vinyl protons of each isomer.

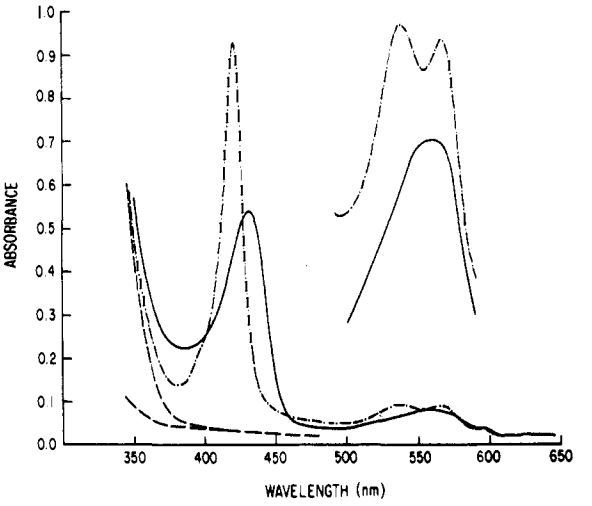

Figure 9. Spectra of chelated protoheme **9** derivatives in 2% Cet-Me_3NBr-0.1 F potassium phosphate buffer at pH 7.3, 25 °C: sodium dithionite at two concentrations (---); after addition of $\mathbf{9}^+Cl^-$ to the excess sodium dithionite (**9**) (—); after addition of 1 atm of CO (**9**-CO) (-·-·-).

The chemical-shift difference is such that the superpositions of doublets resemble triplets.

No splitting of bound imidazole resonances can be found. However, when the asymmetry of the ring is enhanced by substituting for vinyl groups strongly electron-withdrawing acetyl groups, the 2- and 4-bound resonances are distinctly split by 0.01–0.02 ppm, clearly demonstrating the presence of two distinct bonding arrangements.[35] These results serve to characterize the chelated heme-CO complexes employed in our kinetic studies and suggest means of detecting the angle of the imidazole plane of rotation about its Fe-N bond.[35b]

Visible Spectroscopy. Solutions of the hemin compounds (1–20 μM) were prepared in various organic solvents, organic solvent-water mixtures, or in 2–2.5% cetyltrimethylammonium bromide ($CetMe_3NBr$) solutions in aqueous, 0.1 F, phosphate buffer and spectra determined in 1-cm cuvettes. The positions and relative intensities of all peaks were independent of concentration (from 5×10^{-7} to 5×10^{-5} M) in both organic solvents and in $CetMe_3NBr$ suspension, indicating monodisperse hemins or heme compounds. Typical visible spectra are shown in Figure 8 for the chelated pyrroheme **1** as the hemin chloride $\mathbf{1}^+Cl^-$, the deoxy compounds, **1**, the carbon monoxide complex **1**-CO, and the oxygen complex **1**-O_2, and the same series for the corresponding protoheme model compounds, **9**, $\mathbf{9}^+Cl^-$, **9**-O_2, and **9**-CO is shown in Figures 9 and 10. Figure 11 shows the Soret region spectra of the oxygen complex, **1**-O_2, in $CetMe_3NBr$ buffer solution at pH 7.3 and in dimethylformamide. The oxy spectrum in $CetMe_3NBr$ was determined by flash spectroscopy after photodissociation of carbon monoxide. It corresponds closely to that determined by ordinary spectroscopy and shows that the flash photolysis method is detecting reversible oxygenation. However, in this experiment only about 80% yield of the oxy complex **1**-O_2 was achieved as expected from the relative rate constants and concentrations of CO and O_2.

The effect of having the base covalently attached was dramatically shown by the spectra of mesoheme dimethyl ester **3**, the chelated mesoheme **5**, and the dichelated mesoheme **6**. It is remarkable that the spectrum of mesoheme dimethyl ester in aqueous $CetMe_3NBr$ suspension is identical with its spectrum in carefully dried benzene.[36,37] It would appear that water has rather low affinity for hemes and that this affinity is further reduced in the Cet Me_3NBr micelle. The spectra of compounds **1**–**10** are tabulated in Table IV.

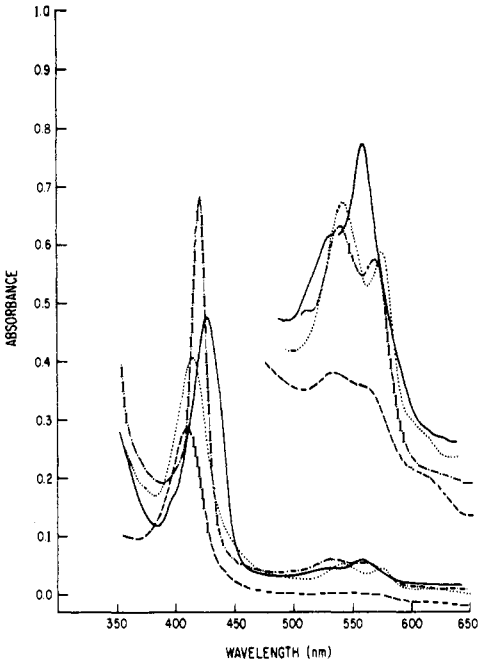

Figure 10. Spectra of **9** derivatives in dimethylformamide at 15 °C as hemin (9^+Cl^-) (---); after reduction with sodium dithionite-crown ether (**9**) (—); after addition of 1 atm of O_2 (**9**-O_2) (···); after flushing the gas phase briefly with CO (**9**-CO) (-·-·-).

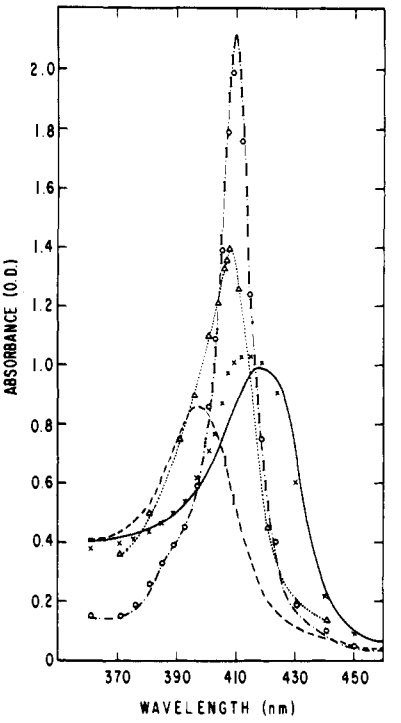

Figure 11. Soret spectra of **1** derivatives taken from absorbance vs. time curves at different wavelengths after flash photolysis in 2% $CetMe_3NBr$-0.1 F potassium phosphate buffer at pH 7.3, along with spectra determined in the usual way. $\mathbf{1}^+Cl^-$ in $CetMe_3NBr$-buffer (---); after titration to **1** with sodium dithionite (—); after addition of 1 atm of CO (-·-·-); spectrum of **1**-O_2 in DMF-H_2O at 15 °C (···). Flash photolysis points in $CetMe_3NBr$ buffer at pH 7.3, 23 °C under 16.6 Torr (2.2×10^{-5} M) CO and 16.6 Torr (3×10^{-5} M) O_2 after a 2000-μs flash: immediately after flash (×); after 10 ms (△); after 2 s (○). These correspond to points at the beginning and end of curve a and at the end of curve b in Figure 12.

Stoichiometry of Oxygenation. We have previously employed mass spectral techniques to show that dioxygen is taken up by a solid film of deoxy-**1** and that the dioxygen is replaced by carbon monoxide.[2a] Similarly, the diimidazole compound **6** was reduced in dry DMF and treated with a known excess of dioxygen in an oxygen-argon mixture of known composition. Before and after equilibrating this mixture with the solution of **6** that had been reduced with Pd and hydrogen, the relative mass spectral peak heights were determined. Then a known amount of carbon monoxide gas was added and the peak height determined again. From the ratios of argon to carbon monoxide or dioxygen peak heights, and the known amounts of gases added, the amount of dioxygen first absorbed and then displaced by carbon monoxide can be determined. These quantities are listed in Table V. Except for the heme being in solution, this experiment was performed exactly as previously described.[2a]

These data clearly show that the reaction with oxygen is completely reversible and has the stoichiometry shown below.

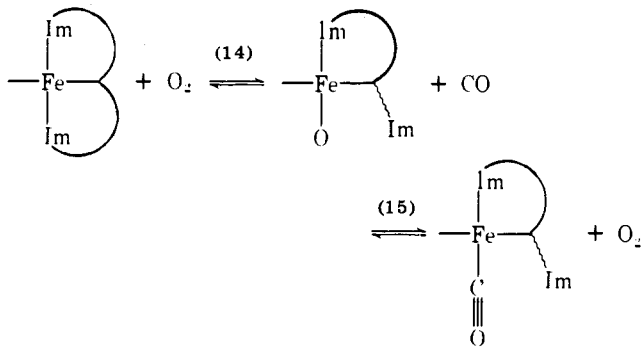

Kinetics and spectroscopic comparisons of **5** and **6** indicate that the second imidazole does not seriously interfere with dioxygen or carbon monoxide binding, **6** reacting only about five times slower with CO than does **5**.

Kinetics. Because the compounds **1**, **5**, and **9** exist in solvents as five-coordinated hemes like myoglobin, react faster with dioxygen than with carbon monoxide, and have photolabile carbon monoxide complexes, the photoflash kinetic techniques applied to hemoproteins[3a] are directly applicable to these compounds. This discovery has allowed the kinetics and equilibria of oxygenation of simple heme compounds to be measured for the first time.[12a,b] In the reaction sequence shown in eq 16 and 17, the rate constant l' for return to HmCO can

$$\mathrm{HmCO} \underset{l'}{\overset{h\nu,\ l}{\rightleftharpoons}} \mathrm{Hm} + \mathrm{CO} \tag{16}$$

$$\mathrm{Hm} + \mathrm{O_2} \underset{k}{\overset{k'}{\rightleftharpoons}} \mathrm{HmO_2} \tag{17}$$

be determined directly following a flash that removes carbon monoxide with a quantum yield of approximately 1. In the presence of dioxygen at appropriate pressures, a biphasic absorbance vs. time curve is observed. An initial, rapid combination rate gives the rate constant k' directly; the ensuing slow rate describes the system's relaxation to HmCO (Figure 12).

Following the rapid reaction of Hm with O_2 (curves a and a'), the HmO_2 returns to HmCO with an observed rate (curves b and b') having a rate constant, k_{obsd}, given by the rate of dissociation of HmO_2 times the fraction of Hm going to HmCO (provided that l is very small compared to k):[3e]

$$k_{obsd} = k\left(\frac{l'[\mathrm{CO}]}{l'[\mathrm{CO}] + k'[\mathrm{O_2}]}\right) \tag{18}$$

This can be rearranged to:

Table IV. Spectra of Model Compounds in Solutions[a]

compd	proximal base	solvent	temp, °C	derivative	Soret	β	α
1$^+Cl^-$	Im	DMF	15	Fe^+Cl^-	392		
1	Im	DMF	15	deoxy	415	548	
1-CO	Im	DMF	15	CO	407	525	558
1-O_2	Im	DMF	15	O_2	404	530	560
3	none	$CetMe_3NBr$	23	Fe(II)	384	529	562
					411		
					439 sh		
3-CO	H_2O	$CetMe_3NBr$	23	CO	403	522	552
5	Im	$CetMe_3NBr$	23	deoxy	417	545	
5-CO	Im	$CetMe_3NBr$	23	CO	410	527	556
6	Im	$CetMe_3NBr$	23	$Fe^{II}Im$	407		
7$^+Cl^-$	Im	$CetMe_3NBr$	23	Fe^+Cl^-	394		
8$^+Cl^-$	Pyr	$CetMe_3NBr$	23	Fe^+Cl^-	393		
8	Pyr	$CetMe_3NBr$	23	deoxy	413		
					425 sh		
8-CO	Pyr	$CetMe_3NBr$	23	CO	408		
9$^+Cl^-$	Im	$CetMe_3NBr$	23	Fe^+Cl^-	403	525	565
					(75)	(7.4)	(6.3)[b]
9	Im	$CetMe_3NBr$	23	deoxy	430		558
					(114)		(13.5)
9-CO	Im	$CetMe_3NBr$	23	CO	420	540	569
					(203)	(16.3)	(15.2)
9$^+Cl^-$	Im	DMF/H_2O (70:30)	15	Fe^+Cl^-	408	540	565
					(90.8)	(7.3)	(6.4)[c]
9	Im	DMF/H_2O (70:30)	15	deoxy	427	530	558
					(124)	(10.6)	(15.4)
9-CO	Im	DMF/H_2O (70:30)	15	CO	420	540	569
					(203)	(15.5)	(13.7)
9-O_2	Im	DMF/H_2O (70:30)	15	O_2	414	543	575
					(121)	(16.5)	(14.2)

[a] Extinction coefficients, mM, in parentheses. [b] A shoulder (ϵ = 4.4) appeared at 610 nm. [c] A shoulder (ϵ = 2.6) appeared at 670 nm.

Table V. Amounts of O_2 Absorbed and Liberated by CO in DMF Solutions of **6** at −45 °C

total heme	4.26 μmol
O_2 absorbed	4.28 μmol
CO absorbed	4.99 μmol
O_2 released by CO	4.56 μmol

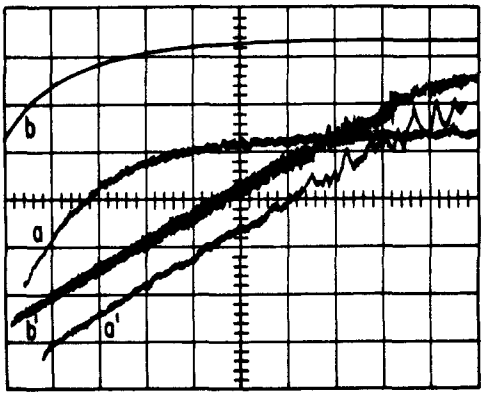

Figure 12. Oscilloscope traces of the 410-nm absorbance vs. time (curved lines) and ln (absorbance$_t$ − absorbance$_\infty$) vs. time (straight lines) after flashing a solution of 4.3 μM chelated mesoheme **5** in 2% $CetMe_3NBr$–0.1 F potassium phosphate buffer having 21 μM O_2 and 35 μM CO concentration (including **5**-CO) at 23 °C. Abscissa: (b) 50 ms/division; (a) 0.5 ms/division; (b′) 20 ms/division; (a′) 0.2 ms/division. Ordinate: (a and b) 0.05 absorbance unit/division; (a′ and b′) 0.5 ln unit/division.

$$\frac{1}{k_{obsd}} = \frac{1}{k} + \frac{k'}{kl'}\left(\frac{[O_2]}{[CO]}\right) \qquad (19)$$

A plot of the reciprocal of the observed rate constant, k_{obsd}, against the ratio of dioxygen to carbon monoxide concentrations then gives an intercept yielding k^{-1} and a slope from which K_{O_2} and thus k' can be obtained. A typical plot of such a set of data is shown in Figure 13. Alternatively, $l'[CO]$ can be determined directly before addition of O_2 and $k'[O_2]$ can be observed directly at the Hm vs. HmCO isosbestic point. These, with k_{obsd}, give k directly.

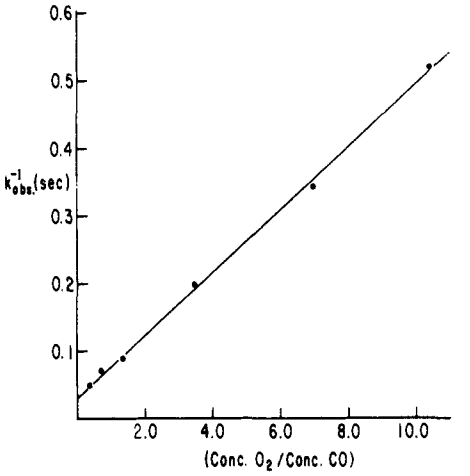

Figure 13. Plots of reciprocal of the slower rate constant observed after photolysis of a solution of **5**-CO in 2% $CetMe_3NBr$ buffer against the ratio of dioxygen to carbon monoxide concentrations (including the CO from **5**-CO).

By observing the biphasic curve (Figure 12) associated with k' and k_{obsd} at different wavelengths, we can obtain spectra of the intermediates. The spectrum of the intermediate oxyheme **1**-O_2 in aqueous $CetMe_3NBr$ suspension, obtained in this way, is shown in Figure 11.

Table VI. Kinetic Constants for Reaction of Dioxygen and Carbon Monoxide with Chelated Heme Compounds at 22 °C

compd	pH	l', $M^{-1}\,s^{-1}$ $\times 10^{-6}$	k', $M^{-1}\,s^{-1}$ $\times 10^{-6}$	k, s^{-1}	K_{O_2}, μM^{-1}	solvent
3[a]	7.3	300[a] (240)[b]	*c*	*c*	*c*	$CetMe_3NBr$
5[c]	7.3	11	22	23	1.0	$CetMe_3NBr$
5		8	53	1700	0.03	toluene-CH_2Cl_2, 90% v/v
6	7.3	2.3	*c*	*c*	*c*	$CetMe_3NBr$
6	7.3	2.5	*c*	*c*	*c*	Triton X-100
7	7.3	26	40	33	1.2	$CetMe_3NBr$
7	5.5	70	40	32	1.2	$CetMe_3NBr$
8	7.3	12	17	380	0.045	$CetMe_3NBr$
9	7.3	4	20	44	0.5	$CetMe_3NBr$

[a] Reference 36. [b] Reference 29. [c] Attempts to study the kinetics of oxygenation were not successful due to oxidation, even in the presence of carbon monoxide. [d] Reference 35.

Kinetic parameters for some of the compounds in Table I are shown in Table VI.

Discussion

In order to produce chelated hemes whose structures correspond as closely as possible to those in natural or reconstituted hemoproteins, we chose to couple potential proximal base side chains to naturally occurring hemes or their derivatives. Because these chelated hemes are prepared by unsymmetrical coupling of a single proximal base chelating arm, we obtain a mixture of two isomeric compounds that we do not separate. Even the dicoupled product, when chelated, produces two isomers (see eq 13). The presence of the two isomers is verified by the two resonances seen for some of the meso protons in the NMR (Figure 3).

We have been unable to crystallize these chelated hemes, perhaps due to the lack of symmetry and the mixtures of compounds. Therefore, we have resorted to other methods of characterization which better characterize the compounds in solution. First, because $\mathbf{9}^+Cl^-$ is prepared in one step from protohemin, there is little need to prove the heme ring structure. Secondly, even in those cases where external base-heme structures are asserted to be characterized by X-ray crystallography, this does not constitute the characterization of the species *in solution*. For example, a crystalline heme-1-methylimidazole compound when dissolved in a $CetMe_3NBr$ suspension or in benzene at 5 μM concentration dissociates almost completely into heme and 1-methylimidazole.[29,37] Such dissociation is less of a problem with chelated hemes having the imidazole arm. Nevertheless, in order to understand the dynamic behavior of chelated hemes toward ligands, we wish to characterize them as completely as possible in solution. NMR spectroscopy is the most definitive method for this purpose.[38]

The NMR spectra of the mono- and dichelated protoheme derivatives **9**-CO and **10**-CO make possible the assignment of the NMR position of every proton in both structures and serve to indicate the basic structure of these compounds. Clearly the coupling reactions have not affected either the heme ring or the vinyl groups. But more importantly, a comparison of these two NMR spectra confirms the conclusion, previously reached from kinetic and visible spectra studies,[12c] that the chelation arm in these CO complexes is completely bound to the iron (within the accuracy of the NMR method). The large chemical shift between iron-bound and unbound side chain protons in **10**-CO is definitive evidence of such binding (Figure 3).

The very close similarity between the visible spectra of the solutions that were characterized by NMR and dilute (micromolar) solutions of these same CO complexes in Me_2SO or in $CetMe_3NBr$ suspension (compare Figures 5 and 9) serves to document our assignment of the chelated structure to these compounds in dilute solution where our kinetic measurements are usually made. Unlike one-to-one mixtures of heme-imidazoles, these chelated hemes show visible spectra which are independent of concentration of base (and heme) from 1 μM to 0.05 M.

The very large differences in the visible spectra[5b] of four-, five-, and six-coordinated hemes sometimes allow ligation of a deoxy chelated heme such as **5** or **9** to be determined directly. In particular, the four-coordinated and six-coordinated hemes have well-defined (but different) α and β bands, whereas five-coordinated hemes such as myoglobin have a single broad band in the α,β region around 520–580 nm (see **3**, **5**, and **6** in Table VI). From the nature of these bands we conclude that monochelated hemes such as **5** or **9** are five-coordinated (high spin) in noncoordinating solvents such as toluene, methylene chloride, DMF, or $CetMe_3NBr$ suspension, but are substantially hexacoordinated (low spin) in solvents such as methanol, dimethyl sulfoxide, or ethers.[36]

Because solvent ligation could compete (in most cases rather weakly)[37] with binding of other ligands such as dioxygen or carbon monoxide, we have preferred solvent systems that do not coordinate with heme iron. The $CetMe_3NBr$ suspension serves to prevent water coordination. In addition, the solubilities of carbon monoxide and dioxygen in the dilute micelle suspension are very likely identical with those in dilute protein solutions. Both the protein and the micelles have hydrophilic exterior and somewhat hydrophobic interiors. It therefore seems reasonable to make no corrections for gas solubilities in these suspensions in making comparisons with hemoprotein solutions. Kinetic behaviors of model compounds toward ligands are not altered by changing the suspending agent from $CetMe_3NBr$ to the nonionic detergent Triton B (see Table VI).

We have shown in another study that the carbon monoxide binding constant for the deuteroheme-imidazole complex (eq 20) is reduced by a factor of 190 upon changing from 1-methylimidazole (R_1 = Me; R_2 = H) to 2-methylimidazole

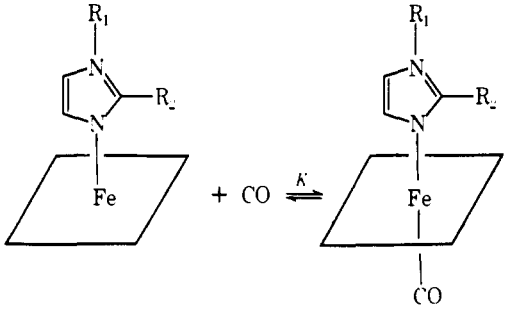

(20)

(R_1 = H; R_2 = Me) in a $CetMe_3NBr$ suspension.[29] The change is exactly the same as that in benzene observed by Rougee and Brault.[39] Because 2-methylimidazole greatly inhibits the binding of a sixth ligand, this result requires that the solvent is not binding to iron in a $CetMe_3NBr$ suspension any more than it is doing in benzene.

Scheme I

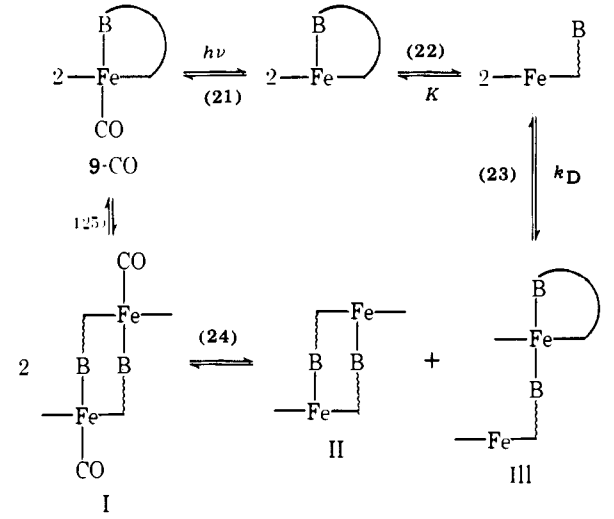

Absence of Polymeric Forms of Chelated Hemes. It has been suggested that chelated hemes such as **9** may disproportionate into either dimeric or polymeric forms in toluene solution.[32] We present the following three observations which clearly demonstrate that such a phenomenon is not a factor in our studies of ferrous chelated hemes, whether under equilibrium or kinetic conditions.

The possible reactions involved in dimerization are shown in Scheme I. It is not possible to distinguish between **9**-CO and a CO dimer (I) by visible spectroscopy. However, as we have shown above, the proton NMR spectrum of **9**-CO provides excellent evidence that the complex indeed exists as the chelated monomer, and not the open-chain dimer (see Figures 3 and 4). The side-chain chemical shifts of the open-chain dimer (I) would be expected to more closely resemble those of the external base complex **11**-CO. The shifts of **9**-CO, especially those for the position labeled 7 in Table III, show that the bonding arrangement is *intra*molecular and relatively rigid in Me_2SO-d_6; similar results have been obtained in benzene-d_6 (not shown). Thus, the chelation arm serves to keep the local concentration of imidazole sufficiently high so that intramolecular binding such as in I is disfavored. The equilibrium in eq 25 lies to the side of the monomer even at normal heme NMR concentrations of 20–30 mM, so dimer formation is certainly not possible in micromolar solutions of chelated hemes.

Two types of deoxy dimers are possible: a completely five-coordinated dimer as in II or a mixture of four- and six-coordinated heme as in III. Again, one would not expect to differentiate II and monomeric **9** by visible spectroscopy. However, it is reasonable to assume that high local concentration of the chelation arm, demonstrated in the CO complex, is still effective in the deoxy form. This precludes existence of II, under equilibrium conditions, at the low heme concentrations employed in visible spectroscopic studies.

The existence of dimers of form III would require a mixture of spectral characteristics quite unlike those of a simple deoxy heme.[32] Such a spectrum has never been observed for our deoxy, unstrained chelated hemes in dilute solution.

Further, this six-coordinated dimerization requires that the product of the equilibrium binding constant of the second base, K_B^B, times the heme concentration exceeds that of the binding constant of the first base, K^B, times the effective local concentration of the chelated base. The value of ~200[36] for the closure equilibrium K (eq 22) and the affinity of imidazole and heme in $CetMe_3NBr$[29] lead to an effective local concentration of the chelated imidazole of >1 M. In benzene, where $K_B^B = 10K^B$, heme concentrations in the millimolar range would be required before substantial amounts of six-coordinated heme would form, consistent with published observations.[32] In $CetMe_3NBr$ suspension, with $K_B^B \simeq K^B$,[29] even higher heme concentrations would be necessary; in either case, these concentrations are far higher than those normally used.

The possibility still remains that dimeric species could be generated transiently in kinetic investigations in solvents, such as benzene, which favor hexacoordination by the base. Again referring to Scheme I, photolysis of **9**-CO leads immediately to deoxy-**9** (eq 21). If reversible loss of base, giving four-coordinated heme, were followed by a rapid dimerization reaction k_D leading to II or III (eq 22 and 23), then the recombination rate of CO would show different kinetics. This dimerization can be excluded on kinetic grounds. At 5 μM concentration of heme, even if k_D were diffusion controlled, the rate of dimer formation would be limited by the chelation equilibrium constant K of at least 200 to $k_D[Hm]^2/K = 10^9(5 \times 10^{-6})^2/200 = 1.2 \times 10^{-4}$ M s^{-1}; this is competing with a CO on rate for five-coordinated heme (at 10^{-4} M CO) of at least $5 \times 10^{-6} \times 10^{-4} \times 10^7 = 5 \times 10^{-3}$ M s^{-1}. But we know from other studies[24] that imidazoles react with hemes with rate constants less than 10^9 M^{-1} s^{-1}.

Therefore, even in solvents which favor dimerization, such processes cannot occur during kinetic experiments, which use low heme concentrations.

The above arguments conclusively show that the dimerization of chelated hemes reported by other laboratories[7,32] has not affected any of our previous work and is not seen in the present work. The use of kinetic methods avoids the problem in *any* solvent, and it is not encountered under equilibrium conditions at the usual low heme concentrations employed.

Approaches toward Preparation of Five-Coordinated Hemes in Solution. Three approaches toward the production of five-coordinated hemes have been developed. The cyclophane protection[5a,40-43] or other steric protection[7,44] of one side of the heme has, in some cases, successfully prevented the second imidazole from complexing with the heme.[43,44] The use of 2-methylimidazole as a sterically hindered base was found to result in almost exclusive formation of five-coordinated heme, and this system was offered as a possible myoglobin model.[45] However, the same steric hindrance that prevented binding a second 2-methylimidazole also reduced the affinity for carbon monoxide[39] compared to the 1-methylimidazole. Furthermore, the kinetics and equilibria of binding of CO to this mixture depend upon the concentration of imidazole, and in such a strained system the reaction with carbon monoxide occurs predominantly by a base dissociation mechanism.[46] This does not mean that ligand affinities of the heme-2-methylimidazole complex cannot be obtained. However, they are not observed directly but are obtained by extrapolating to high concentrations of 2-methylimidazole (e.g., above its solubility in benzene).[29,46]

The third method, that of covalently attaching the proximal base to the heme,[2a] has none of the drawbacks of using external bases as proximal ligands due to the neighboring group or chelation effect that maintains a very high local concentration of base.

The enormous advantage of having this local concentration at an actual imidazole concentration of 5 μM is obvious from the above discussion of dimerization.

We have recently been able to derive (by an extrapolation) the rate constant of carbon monoxide reaction with the 1-methylimidazole-mesoheme complex (reaction 26) which is essentially identical with the rate of reaction with **5** (reaction 27). The off rates are also very similar. Therefore, the chelation does not affect this single step as compared to external base-heme mixtures unless the chelation introduces some steric strain.

Chelated hemes, having the same conformation and five-

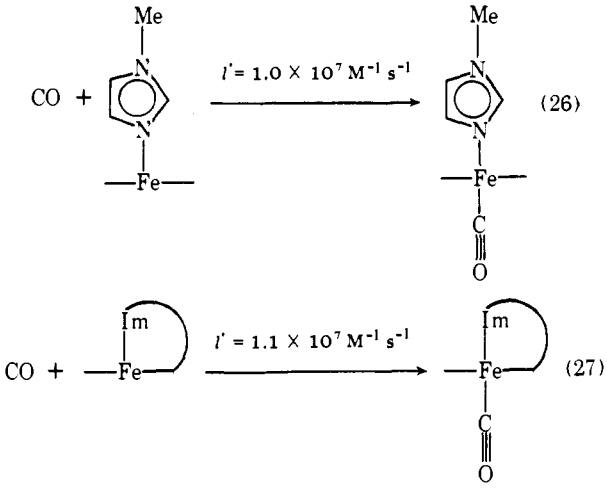

coordinated ligation as does hemoglobin or myoglobin, optimize the conditions for simple dynamic reversible ligation such as oxygenation.[2a,7b]

Characterization of a Reversibly Formed Oxygen Complex. One of the advantages of preparing model compounds from protoheme or mesoheme is that the visible spectra of their derivatives match exactly those of the hemoproteins themselves. A comparison of the spectrum of the dioxygen complex **9**-O_2 in DMF (Figure 8) with that of hemoglobin-O_2 reveals an identity in the Soret and the visible bands in these two compounds.

That carbon monoxide displaces 1 equiv of dioxygen from a solution of **6**-O_2 in DMF is *very strong* evidence for reversible oxygenation rather than oxidation. The flash photolysis of a chelated heme-CO complex in the presence of dioxygen is itself definitive evidence for oxygenation. After photolysis of the carbon monoxide complex **1**-CO, the immediately observed spectrum corresponds to the deoxy form **1**, which changes to the spectrum corresponding to the oxy complex **1**-O_2 at rates that are proportional to dioxygen concentration. Subsequently, the spectrum returns to that of the carbon monoxide complex **1**-CO at rates that are dependent upon both dioxygen and carbon monoxide concentration. These observations are consistent with reversible oxygenation and are very difficult to explain in any other way. These processes are also identical with those which occur with myoglobin except for the actual rate constants.

Perhaps the most interesting demonstration of an oxy complex as contrasted to the oxidized iron is the fact that the oxy complex of chelated protoheme can be prepared in the presence of a reducing agent. In polar aprotic media such as dimethylformamide, the 18-crown-6 complex of sodium dithionite rapidly reduces the Fe(III) form of chelated protoheme.[47]

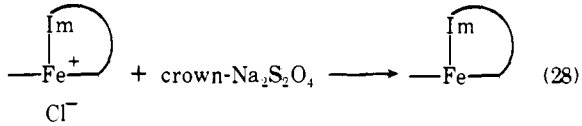

In the presence of excess reducing agent, the addition of dioxygen at 25 °C results in the formation of the oxy complex **9**-O_2, as indicated by its visible spectrum (identical with that shown in Figure 9). The crown ether–sodium dithionite compound does not react with dioxygen under these conditions. Therefore, the spectrum observed when dioxygen is added to this solution cannot correspond to an Fe(III) compound because the excess reducing agent would immediately reduce the Fe(III).

These observations, and the mass spectroscopic identification of dioxygen gas that is displaced from the oxy complex **6**-O_2 with CO, leave little doubt as to the identity of our oxy complexes **1**-O_2, **5**-O_2, **6**-O_2, and **9**-O_2. Since our first report of this complex,[2a] its existence has been independently confirmed[18] and many other dioxygen complexes of simple unprotected heme compounds have been reported.[5b,6]

Chelated Protoheme, an Accurate Model of R-State Hemoglobin. We have previously employed mesoheme or pyrroheme derivatives and have compared them with hemoproteins reconstituted with the corresponding hemes. In this work we report a very simple synthesis of monochelated protoheme **9**, which has the same electronic properties as the heme in most hemoproteins. Not surprisingly, the spectral properties of this compound in $CetMe_3NBr$ suspension as the deoxy (**9**), oxy (**9**-O_2), and carbonmonoxy (**9**-CO) derivatives correspond almost exactly with those of hemoglobin. A comparison of the kinetics and equilibria of reactions of this compound with those of R-state hemoglobin are included in Table VII. It is quite clear that in $CetMe_3NBr$ suspension not only the binding constants for dioxygen but the on and off rates are rather close to those of R-state hemoglobin.

Because the pressure for half-saturation of heme compounds is solvent dependent, decreasing as CO solubility increases, it is possible to achieve situations in which the $P_{1/2}^{CO}$ for a model compound is lower than that for hemoglobin. For example, chelated mesoheme **5** has a $P_{1/2}^{CO} = 4 \times 10^{-4}$ Torr in toluene, while in $CetMe_3NBr$ suspension the $P_{1/2}^{CO}$ of chelated mesoheme **5** is 10^{-3} Torr, almost the same as that of R-state hemoglobin. With solvent changes the variations in $P_{1/2}^{CO}$ are only factors of about 3 to 7, depending upon the structure of the hemes. Owing to these variations in solubility, we prefer to make the protein comparison in aqueous suspension. The heme in hemoglobin is held in a "micelle" of protein, whereas in $CetMe_3NBr$ the heme is contained in a $CetMe_3NBr$ micelle. At the low concentration of heme used in titration or kinetic studies, the CO is in the water and not in the protein or $CetMe_3NBr$ micelle. Therefore, it is logical to consider the CO activity as identical in these two systems.

The conclusion is that both dioxygen and carbon monoxide bind to R-state hemoglobin without serious interference by the protein,[12b] its function being the maintenance of five-coordinated heme. By synthetically maintaining five-coordinated protoheme, we reproduce both the spectral and kinetic properties of this protein in the R state. This leaves chelated protoheme as the *only* model system that has displayed the same ligation behavior as hemoproteins in both dioxygen and carbon monoxide binding. Modeling of the factors that change this basic five-coordinate protoheme behavior to the kinetic behavior of T-state hemoglobin and other hemoproteins is discussed elsewhere.[29,36]

Reversible Oxygenation of Chelated Hemes at Room Temperature. The first study of reversible oxygenation of chelated hemes was carried out at −45 °C, and it was reported that these compounds were not stable toward oxidation at room temperature.[2b] Some synthetic heme compounds having one side protected by cyclophane[40,41] or bulky groups[44] were reported to undergo reversible oxygenation at room temperature. But such steric protection is *not necessary* for reversible oxygenation at room temperature. The chelated hemes **1**, **5**, **9**, etc., are all reversibly oxygenated at room temperature by reversibly converting the deoxyheme to the carbon monoxide complex. For example, the spectral intermediate **1**-O_2 is an oxyheme obtained by flashing CO off a solution of 5 μM **1**-CO in the presence of dioxygen. Depending upon the relative concentrations of O_2 and CO, this oxyheme **1**-O_2 returns to carboxyheme **1**-CO with half-times of from 0.05 to 1 s, sufficient to make many kinds of measurements on these solutions. Each point on the **1**-O_2 spectrum in Figure 11 is a separate reversible oxygenation of the same solution of **1**. Clearly, reversible oxygenation can be repeated many times at 25 °C without appreciable oxidation. Our observation that (at −45 °C) 1 equiv

Table VII. Comparison of Spectroscopic and Kinetic Properties of Hemoglobin and Chelated Protoheme **9** at 20 °C[a]

compd	Soret	β	α	rate constants: on, $M^{-1}\,s^{-1}$	rate constants: off, s^{-1}	equilibrium constant, M^{-1}
Hb	430 (133)[b]		555 (12.5)			
9	430 (114)		558 (13.5)			
$Hb(CO)_4$	419 (191)	540 (13.4)	569 (13.4)	6×10^6	0.009	7×10^8
9-CO	420 (203)	540 (16.3)	569 (15.2)	6×10^6	0.007[c]	6×10^8
$Hb(O_2)_4$	415	541 (13.8)	577 (14.7)	3×10^7	50[d] 10[e]	$1\text{–}6 \times 10^5$
9-O_2[f]	414 (121)	543 (16.5)	575 (14.2)	2×10^7	44	5×10^5

[a] Chelated protoheme was suspended in 2% cetyltrimethylammonium bromide–phosphate buffer at pH 7.3. [b] Extinction coefficients, millimolar, in parentheses. Those for Hb are from ref 3d. [c] At 22 °C.[48a] [d] At pH 5.[48b] [e] At pH 9 [48b] [f] Static visible spectra determined in 70:30 DMF/H_2O.

of oxygen is absorbed selectively from a dioxygen–argon mixture by a solution of **6**, and reevolved with simultaneous disappearance of 1 equiv of carbon monoxide, all quantitatively identified by mass spectroscopy, is the most definitive evidence that dioxygen is reversibly bound in a solution of a heme model compound. The identity of the visible spectrum of this dioxygen complex to those observed by flash spectroscopy lends strong evidence for the kinetic oxygenation that we report here and elsewhere.

A second method of accomplishing reversible oxygenation involves the use of a selective reductant that reduces any heme which gets oxidized by dioxygen without reducing dioxygen itself. We have prepared an 18-crown-6 complex of sodium dithionite that reduces hemins effectively and rapidly, but reacts very slowly with dioxygen in aprotic solvents such as DMF, Me_2SO, and methylene chloride.[47] Using this reducing agent it is possible to prepare, e.g., **9**-O_2 directly at 25 °C in an air-saturated solution of **9**$^+Cl^-$ in DMF by simply adding a solution of the crown ether–dithionite reducing agent. The

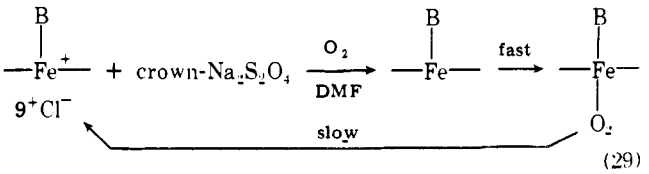

(29)

success of this method depends upon the absence of protic solvents that are required for the reduction of O_2 by dithionite and upon the rather slow oxidation of **9** in DMF or Me_2SO solution. Therefore, this method is not effective at a high concentration of heme or in protic solvents.

The oxygenation of simple hemes has several advantages. First, because steric protection is absent, the effects of solvent or extra side chains in intimate contact with the Fe–CO structure can be studied. Secondly, synthetic problems are simplified because steric protection does not have to be incorporated into each new heme. But, importantly, the model compounds prepared from protohemin have the same structure and thus the same spectra as do hemoproteins. This makes possible the study of subtle changes in spectra of hemoproteins that result from changes in protein structure.[35b]

One difference between simple unprotected heme model systems and those that have steric protection[7] is that the protected hemes can be oxygenated at high concentration and their dioxygen complexes are stable for long periods, whereas those of unprotected hemes are not. For some purposes such stability is required, but kinetics and equilibria of oxygenation can be accomplished at room temperature without this protection.

Nature of the Iron–Dioxygen Bond. Studies of solvent effects on dioxygen binding to chelated hemes suggested a polar form $Fe^{\delta+}\text{–}OO^{\delta-}$ for the oxyheme structure,[19b,49,50] which is also consistent with the O–O stretching frequency of oxyhemoglobin and myoglobin.[51] Further studies of solvent and electronic effects on both CO and O_2 binding dynamics that confirm this conclusion will be reported elsewhere.

Conclusion

Convenient syntheses of hemoprotein model compounds having a covalently attached imidazole arm (chelated hemes) have been described. The chelated protoheme model has been characterized in solution by NMR and simultaneous visible spectroscopy. Imidazole chelated protoheme displays spectroscopic properties and kinetics and equilibria for CO and O_2 binding that are almost identical with those of R-state hemoglobin.

Experimental Section

Protohemin chloride (Sigma or Calbiochem), cetyltrimethylammonium bromide (Sigma), and $Na_2S_2O_4$ (J. T. Baker) were used as received. All solvents were reagent grade. Pyridine was distilled from CaH_2. CO and O_2 were obtained from Matheson Gas Products. Chromatography was performed on silica gel plates (Eastman No. 13181) or on silica gel (Baker) columns. Deuterated solvents were from Stohler Isotope Chemicals.

Visible spectra were determined on a Cary 15 spectrophotometer. Special clear Dewar flasks equipped with a gaseous nitrogen cooler were used for low-temperature spectra.

Nuclear magnetic resonance spectra were determined on a Varian HR-220 spectrometer equipped with Nicolet TT-100 pulse/Fourier transform. Three-four kilohertz sweep widths and 4–8K data points were used, and all shifts are reported downfield of internal Me_4Si. Solutions were prepared 25–40 mM in Me_2SO-d_6 as follows. The hemin was weighed into a precision NMR sample tube, which was closed with a silicone septum. The tube was evacuated via syringe needle and filled with CO or argon, then solvent. Reduction of the hemin was accomplished by addition of 5–10 μL of a D_2O solution saturated with $Na_2S_2O_4$. Aliquots of CO or other ligands could then be added via microliter syringe, and the titrations followed by NMR.

To facilitate identification of the resulting complexes, a simple method was devised to measure visible spectra of samples in the NMR tube. A bored-out vortex plug was fitted midway down the tube. On this rested a 2-cm sleeve of precision glass tubing (Wilmad No. 520-3) that fit the sample tube to leave a 0.04-mm annular space. A stable smear was formed in this annular space, which was equilibrated with the rest of the solution by shaking so that the sleeve slid back and forth in the NMR tube. The use of lenses allowed visible spectra to be measured through this smear on the Cary 15. The visible spectra so obtained were identical with those obtained in dilute solution.

Solutions for Flash Photolysis or Spectroscopic Studies. Kinetics of reaction of the hemoprotein active-site compounds used here were carried out on the same concentrations of solutions and in the same tonometer systems as were used for equilibrium spectroscopy. The heme concentrations were 10^{-6} to 10^{-5} M, in $CetMe_3NBr$ (2%) suspension containing 0.1 M buffer, or in organic or aqueous organic solvents. Some recent batches of $CetMe_3NBr$ (Sigma, Aldrich) precipitated from 2% solutions suggesting that older batches are mixtures with perhaps differing chain lengths.

Two kinds of tonometers have been developed for use with aqueous or partially aqueous systems. For flash photolysis studies, the tonometer shown in Figure 14A was used. This consists of a 1-cm^2 Pyrex cuvette appended to a 100-mL bulb (130 mL total volume), to which is attached a holder for the Applied Science Laboratories W-10 septum (Catalog No. 15443) and a three-way vacuum stopcock. Five milliliters of the $CetMe_3NBr$ buffer or aqueous organic solvent was placed in the tonometer and about 0.01 mg of the requisite heme in about 3 μL of methanol was added. The resulting solution was freeze-pump-thaw degassed three times and 1-2 μL of a degassed solution of 5 mg of sodium dithionite in 5 mL of water was added. For CO studies excess sodium dithionite was added until a dithionite absorption of about 0.5 at 350 nm was observed. When oxygen studies were planned, careful titration to complete heme reduction (monitored in the Soret region) was achieved without appreciable absorption increase at 350 nm. Alternatively, excess dithionite was destroyed, without deleterious effect on the heme, by adding a small amount (<0.5 mg) of hexachloroethane in 1 to 2 μL of CH_2Cl_2 or methanol. The probable course of the reaction (eq 30) produces no interfering products.

$$S_2O_4^{2-} + Cl_3CCCl_3 \rightarrow 2Cl^- + Cl_2CCCl_2 + 2SO_2 \quad (30)$$

After determining the UV-visible spectrum, the appropriate kinds and volumes of gases (CO, O_2, etc.) were injected through the septum using gas-tight syringes, and the tonometer solution was equilibrated with the gas by vigorous shaking at 25 °C, placed in the spectrophotometer or the flash photolysis apparatus, and flashed to obtain kinetics of reaction with CO, O_2, etc. or the spectra were determined. Spectra were usually determined before and after kinetic studies.

In those cases where anhydrous organic solvents were used, a newly developed crown ether-sodium dithionite complex[47] or Pd/C with calcium hydride[12b] was employed.

A simple and convenient method of studying hemes in solution without a gas phase employed the tonometer in Figure 14B. The tonometer neck was made so that the W-10 septum described above was a close, but sliding, fit. A small glass bead was added to the tonometer for stirring, and the tonometer was filled to just overflowing with the buffer solution, organic solvent, or solvent mixture. A thin gage needle was inserted through a septum; then, using the tool shown with the tonometer, the septum was forced into the neck the desired distance and the needle removed. By positioning the septum toward the bottom of a 4-cm neck, as much as 2 mL of solution would be added to the heme solution tonometer by forcing the septum upward as solution was added. This made titrations under anaerobic conditions very convenient. If this was done properly no gas bubbles appeared. To this solution was added via microliter syringe 1-3 μL of a 5% sodium dithionite solution so as to produce an absorption of approximately 0.5 at 350 nm. Approximately 0.01 mg of the hemin chloride of interest was dissolved in 2-5 μL of methanol and added to the tonometer to produce the deoxyheme directly. This method avoids the production of the dithionite plus dioxygen reaction intermediates in the presence of the heme or hemin. The excess sodium dithionite was either left in the tonometer for carbon monoxide, etc., studies, or removed by reaction with added CCl_3CCl_3 if it would interfere. For quantitative carbon monoxide or dioxygen studies, saturated solutions of these gases in the same solvent were added with syringes.

Kinetic Studies. In a typical kinetic experiment, a solution of about 3 μM 7^+Cl^- was degassed and reduced by titration with sodium dithionite in the large tonometer as described above. Successive aliquots of carbon monoxide gas were added with a gas-tight syringe (volume corrected for temperature and pressure). After each equilibration (10-min shaking), the tonometer was placed in the flash photolysis apparatus previously described,[12b] then flashed with a 100-400-μs flash. The absorbance change was recorded on a storage oscilloscope either as A vs. t or ln $(A - A_\infty)$ vs. t, using a specially designed analog processing device.[52] Aliquots of dioxygen gas were added, equilibrated, flashed, and recorded in the same manner, using appropriate time scales.

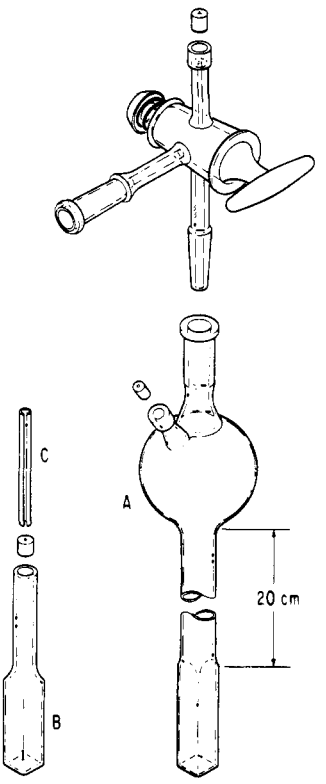

Figure 14. Tonometers for spectroscopic and kinetic studies. B is a 6-mL liquid phase tonometer of variable size and A is a 130-mL gas-liquid tonometer for vacuum line methods.

The combination rate constants for carbon monoxide, l', and for dioxygen, k', were obtained directly by dividing the observed pseudo-first-order combination rate by the appropriate gas concentration,[53] taking into account the CO flashed off the heme. The dioxygen dissociation rates were obtained by the intercept method of Gibson.[3e,54] The absorbance vs. time plots, shown in Figure 12, and the pseudo-first-order rate constants so obtained were reproducible to ±5% for repetitive flashes of the same sample. Sample-to-sample reproducibility with this system was found to be ±10%. We have recently assembled a laser flash photolysis apparatus[29] in which 10-20 kinetic runs are computer averaged to yield a higher signal-to-noise ratio and kinetic constants with standard deviations of ±2% on successive runs on one sample. Reproducibility of complete experiments is ±10% for observed rates of $<10^3$ s^{-1} and ±20% for observed rates of $\geq 10^4$ s^{-1}. Several rate constants measured with the analog device were confirmed by this new system to lie within the stated error limits.

Mass Spectral Determination of O_2 and CO Binding Stoichiometry. A solution of 5 mg of 6^+Cl^- in 18 mL of anhydrous dimethylformamide was reduced with Pd black/calcium hydride[12b] and decanted anaerobically from the catalyst into a preweighed special flask having known volume and a calibrated gas inlet port. The 14.34 g of solution in the flask was subsequently shown by the pyridine hemochrome method to contain 4.26 μmol of **6**. Admitting successively known volumes of a mass spectrally analyzed argon-dioxygen mixture and then carbon monoxide to the solution and, after mixing the solution upon each addition at −45 °C, taking gas samples for analysis allowed the number of moles of dioxygen absorbed and released upon CO addition to be determined. The gas analysis, reaction flask, and gas handling methods were exactly those previously described.[55] The results are listed in Table V.

1-Methylimidazole (Aldrich) was distilled at reduced pressure. Imidazole and 2-methylimidazole (Aldrich) were twice recrystallized from benzene. 1,2-Dimethylimidazole (Aldrich) was used as received. Compounds **1**, **2**, **3**, **6**, and **11** were obtained from a previous study.[12b,c,35] 3-(3-Pyridyl)propanol (Aldrich) and 3-(2-pyridyl)propanol (Aldrich), distilled from calcium hydride, had NMR spectra consistent with their structures.

1-(3-Aminopropyl)imidazole (**11**) was synthesized by the method of Schwan:[56] NMR δ 2.5 (2, NH_2), 2.5 (t, 2 H, CH_2), 1.80 (q, 2 H,

CH_2), 3.94 (t, 2 H, CH_2), 7.61 (s, 1 H, H_2), 7.01 (s, 1 H, H_4), 7.09 (s, 1 H, H_5).

Mesoporphyrin dimethyl ester (**3P**) was prepared by the method described by Falk[57] and partially hydrolyzed as follows.

Mesoporphyrin Monomethyl Ester (4P). Mesoporphyrin dimethyl ester (**3P**), 200 mg (0.345 mmol), was dissolved in 20 mL of 4 N hydrochloric acid and stirred for 12 min at room temperature. Two hundred milliliters of distilled water was added and the aqueous layer extracted repeatedly with 30-mL portions of methylene chloride until no further porphyrin was obtained. The combined organic extracts were washed twice with 2% aqueous sodium bicarbonate, twice with distilled water, and dried over anhydrous potassium carbonate. The mixture of porphyrins was dissolved in methylene chloride–tetrahydrofuran (95:5) containing 0.5% triethylamine and chromatographed on silica gel. Elution with this solvent mixture cleanly separated mesoporphyrin dimethyl ester, leaving a mixture of mesoporphyrin monoacid monomethyl ester and mesoporphyrin diacid on the column. Elution with a methylene chloride–methanol mixture (4:1) separated mesoporphyrin monomethyl ester, monoacid. The recovered mesoporphyrin dimethyl ester was recycled through the partial hydrolysis, and the very small amount of remaining mesoporphyrin diacid was discarded with the silica gel. The yield was approximately 30% per hydrolysis cycle; 200 mg of mesoporphyrin dimethyl ester yielded 130 mg of mesoporphyrin monomethyl ester, monoacid after three iterative hydrolyses: IR, ester and acid carbonyl absorption at 1730 cm^{-1}. The visible spectrum is identical with that of mesoporphyrin IX: NMR ($CDCl_3$) δ 10.04 (s, 4 H, meso), 4.40 (t, 4 H, propionate), 4.07 (q, 4 H, Et), 3.69–3.60 (m, 15 H, methyls), 3.26 (t, 4 H, propionate), 1.96 (t, 6 H, Et), −3.92 (s, 2 H, pyrrole H).

Mesohemin Mono-3-(1-imidazolyl)propylamide, Monomethyl Ester (5^+Cl^-). Mesoporphyrin monomethyl ester, monoacid (**4P**), 25 mg (42.6 μmol) was dissolved in 10 mL of anhydrous methylene chloride under an argon atmosphere. The mixed anhydride was formed quantitatively by adding 43 μmol of pivalyl chloride and stirring for 1 h, and then was reacted without purification with 6.25 mg (50 μmol) of 1-(3-aminopropyl)imidazole (**11**). The mixture was stirred overnight. The solvent was evaporated with the crude product chromatographed on silica gel. Elution with methylene chloride–methanol (4:1) afforded the final product (5P): yield, 22 mg (75%); NMR ($CDCl_3$) δ 10.1 (s, 4 H, meso), 10.04 (s, 1 H, amide), 7.1, 6.7, 6.2 (3 s, 3 H, imidazole), 3.5–3.6 (m, 15 H, methyls); IR ester carbonyl absorption at 1730 cm^{-1}, amide carbonyl absorption at 1662 cm^{-1}. The visible spectrum was identical with that of the precursor.

The porphyrin was converted to the hemin chloride by the method of Falk.[57] Chromatography on silica gel, eluting with methylene chloride–methanol (4:1) containing 0.5% triethylamine, yielded the final product (5^+Cl^-). This compound can also be obtained by hydrogenation of 9^+Cl^-.

Mesohemin Mono-3-(3-pyridyl)propyl Ester, Monomethyl Ester (8^+Cl^-). An anhydrous slush of *p*-toluenesulfonic acid in methylene chloride was prepared by placing approximately 50 g of *p*-toluenesulfonic acid monohydrate (Aldrich, T3592) and 150 mL of methylene chloride in the pot of a Soxhlet extractor and refluxing the azeotrope over solid CaH_2 contained in the thimble for 6 h. Mesoporphyrin monomethyl ester (**4P**), monoacid, 30 mg (51.7 μmol), was dissolved in 20 mL of *p*-toluenesulfonic acid saturated anhydrous methylene chloride. Seven microliters (51.7 mmol) of 3-(3-pyridyl)propanol was added. The reaction mixture was heated to reflux. The methylene chloride was refluxed over fresh molecular sieves before returning it to the pot. Reflux was continued for 24 h. The reaction mixture was extracted three times with 2% aqueous bicarbonate and three times with distilled H_2O. The crude product was chromatographed on silica gel, eluting with methylene chloride–methanol (95:5) containing 0.5% triethylamine. Switching solvents to methylene chloride–methanol (4:1) eluted a second smaller fraction. The yield of mesoporphyrin mono-3-(3-pyridyl)propyl ester (**8P**) was 18 mg (50%): NMR ($CDCl_3$) δ 10.08 (s, 4 H, meso), 8.07 (m, 2 H, Pyr 2, 6 H), 6.42 (m, 2 H, Pyr 4, 5 H), 4.45 (t, 4 H, propionate), 4.09 (q, 4 H, Et), 4.00 (t, 2 H, propyl), 3.5–3.6 (m, 15 H, methyls), 3.31 (t, 4 H, propionate), 2.00 (t, 2 H, propyl), 1.88 (t, 6 H, Et), 1.52 (m, 2 H, propyl), −3.79 (s, 2 H, pyrrole H). Eight milligrams of starting mesoporphyrin monomethyl ester, monoacid was recovered.

Iron was inserted in the usual manner. The hemin solution in chloroform was washed with 0.1 N hydrochloric acid, dried, and evaporated. Chromatography on silica gel, eluting with CH_2Cl_2–CH_3OH (4:1) containing 0.5% triethylamine, afforded the final product (8^+Cl^-) in a yield of 16 mg (79%): IR ester carbonyl absorption at 1725 cm^{-1}.

This compound (8^+Cl^-) can also be prepared in good yield by the pivalyl chloride method.

Protohemin Mono-3-(1-imidazolyl)propylamide, Monomethyl Ester (9^+Cl^-). To a three-necked, round-bottomed flask equipped with condenser, rubber septum, magnetic stirring bar, and dry atmosphere was added 30 mL of dry pyridine and 0.5 g (0.77 mM) of protohemin chloride (Calbiochem). The flask was cooled in an ice bath and the pivalyl chloride (1.40 mM) added via syringe over 20 min. Conversion to anhydride can be followed by quenching aliquots with methanol and chromatographing the product on TLC plates. Development with 9:1 CH_3Cl–MeOH shows the dimethyl ester of hemin with R_f 0.55, side products at R_f 0.2.

A 10% solution of 1-(3-aminopropyl)imidazole (**11**) (0.63 mM) in pyridine was added to the anhydride solution in 20 min with stirring. Conversion to the monoamide (9^+Cl^-) (R_f 0.37) and diamide (10^+Cl^-) (R_f 0.18) was followed by TLC as described above.

Following the amine addition, 10 mL of MeOH was added, the solution was stirred 10 min, and the volatiles were removed in a rotatory evaporator. The crude product was dissolved in chloroform, washed with dilute hydrochloric acid, and applied to a silica gel column packed in $CHCl_3$–1% Et_3N. Elution with 9:1:0.1 $CHCl_3$–MeOH–Et_3N provided the dimethyl ester of hemin first, followed by the monoamide monoester (9^+Cl^-). With some batches of protohemin chloride, fast eluting impurities appeared. These could be removed by chromatography with a 95:5 chloroform–formic acid eluent, which slows elution of the imidazole derivatives, followed by the elution described above. Analysis of 9^+Cl^-: Calcd for $C_{41}H_{43}N_7O_3FeCl$: C, 63.69; H, 5.61; N, 12.67. Found: C, 63.88; H, 5.71; N, 12.62. NMR (Me_2SO, Fe(III) dicyano complex): The imidazole protons were at δ 7.77, 7.41, and 6.83, and those of the propyl side chain at 4.20, 2.74, and 1.88. The remaining heme substituents showed resonances consistent with the assignment for dicyano protohemin:[58] IR ($CHCl_3$) 3020, 1730, 1650 cm^{-1}.

When the reaction mixture was quenched with water instead of methanol, the monoacid monoamide was obtained.

References and Notes

(1) The National Institutes of Health supported this research (Grant No. HL 13581) and the NMR facilities which were used (Grant No. RR 00708).
(2) Some of the results presented here were previously communicated in preliminary form: (a) Chang, C. K.; Traylor, T. G. *Proc. Natl. Acad. Sci. U.S.A.* **1973**, *70*, 2647–2650. (b) Chang, C. K.; Traylor, T. G. *J. Am. Chem. Soc.* **1973**, *95*, 5810–5811.
(3) (a) Antonini, F.; Brunori, M. "Hemoglobin and Myoglobin and Their Reactions with Ligands"; North Holland Publishing Co.: Amsterdam, 1971; p 287; (b) p 350; (c) p 13; (d) p 19; (e) p 197.
(4) (a) Perutz, M. F. *Nature (London)* **1970**, *228*, 726–739. (b) Heidner, E. J.; Ladner, R. C.; Perutz, M. F. *J. Mol. Biol.* **1976**, *104*, 707–722. (c) Perutz, M. F. *Br. Med. Bull.* **1976**, *32*, 195–208. (d) Perutz, M. F.; Muirhead, H.; Cox, J. M.; Goaman, L. C. G. *Nature (London)* **1968**, *219*, 131–139.
(5) (a) Diekmann, H.; Chang, C. K.; Traylor, T. G. *J. Am. Chem. Soc.* **1971**, *93*, 4068–4070. (b) Traylor, T. G. In "Bioorganic Chemistry"; van Tamelen, E., Ed.; Academic: New York, 1978; Vol. IV, p 437.
(6) Basolo, F.; Hoffman, B. M.; Ibers, J. A. *Acc. Chem. Res.* **1975**, *8*, 384–392.
(7) (a) Collman, J. P. *Acc. Chem. Res.* **1977**, *10*, 265–272. (b) Collman, J. P.; Brauman, J. I.; Doxsee, K. M.; Halbert, T. R.; Hayes, S. E.; Suslick, K. S. *J. Am. Chem. Soc.* **1978**, *100*, 2761–2766.
(8) (a) Wang, J. H. In "Oxygenases"; Hayaishi, O., Ed.; Academic: New York, 1970; p 499; (b) p 503. (c) Wallace, W. J.; Maxwell, J. C.; Caughey, W. S. *Biochem. Biophys. Res. Commun.* **1974**, *57*, 1104–1110.
(9) Cohen, I. A.; Caughey, W. S. *Biochemistry* **1968**, *7*, 636–641.
(10) Chang, C. K.; Powell, D.; Traylor, T. G. *Croat. Chem. Acta* **1977**, *49*, 295–307.
(11) Chin, D.; Del Gaudio, J.; La Mar, G. N.; Balch, A. *J. Am. Chem. Soc.* **1977**, *99*, 5486–5488.
(12) (a) Chang, C. K.; Traylor, T. G. *Biochem. Biophys. Res. Commun.* **1975**, *62*, 729–735. (b) Chang, C. K.; Traylor, T. G. *Proc. Natl. Acad. Sci. U.S.A.* **1975**, *72*, 1166–1170. (c) Geibel, J.; Chang, C. K.; Traylor, T. G. *J. Am. Chem. Soc.* **1975**, *97*, 5924–5926.
(13) (a) Lautsch, W.; Wiener, B.; Zschendenlain, P.; Kraege, H. J.; Bande), W.; Günther, D.; Schulz, G.; Gnichtel, H. *Kolloid-Z.* **1958**, *161*, 36–49. (b) Lautsch, W.; Pasedag, R.; Sommer, I.; Julius, H. J.; Boederfield, E. *Chimia* **1959**, *13*, 129–142. (c) Lautsch, W.; Gehrmann, R.; Pasedag, R.; Prater, K. *Chem. Ber.* **1957**, *90*, 470–481.
(14) Losse, G.; Müller, G. *Z. Physiol. Chem.* **1982**, *327*, 205–216.
(15) (a) Warme, P. K.; Hager, L. P. *Biochemistry* **1970**, *9*, 1599–1605; (b) *Ibid.*, 1606–1614.
(16) van der Heijden, A.; Peer, H. G.; van den Oord, A. H. A. *J. Chem. Soc., Chem. Commun.* **1971**, 369–370.
(17) Laplawy, M. T.; Jones, D. S.; Kenner, G. W.; Sheppard, R. C. *Tetrahedron* **1960**, *11*, 39–51.

(18) Almog, J.; Baldwin, J. E.; Dyer, R. L.; Huff, J.; Wilkerson, C. J. *J. Am. Chem. Soc.* **1974**, *96*, 5600–5601.
(19) Scheer, H.; Katz, J. J. In "Porphyrins and Metalloporphyrins"; Smith, K., Ed.; Elsevier: New York, 1975.
(20) Abraham, R. J.; Eivazi, F.; Pearson, H.; Smith, K. *J. Chem. Soc., Chem. Commun.* **1976**, 689–699.
(21) Janson, T. R.; Katz, J. J. *J. Magn. Reson.* **1972**, *6*, 209–220.
(22) Faller, J. W.; Sibert J. W. *J. Organomet. Chem.* **1971**, *31*, C5–C8.
(23) Although 2-methylimidazole competes well with other bases for four-coordinated heme, it binds poorly to five-coordinated heme, making the Me_2SO-heme-CO stability comparable to that of 2-MeIm-heme-CO in Me_2SO as solvent.
(24) Goff, H.; La Mar, G. N. *J. Am. Chem. Soc.* **1977**, *99*, 6599–6606.
(25) Abraham, R. J.; Fell, S. C. M.; Smith, K. M. *Org. Magn. Reson.* **1977**, *9*, 367–373.
(26) Dwyer, P. N.; Madura, P.; Scheidt, W. R. *J. Am. Chem. Soc.* **1974**, *96*, 4815–4819.
(27) Satterlee, J. D.; La Mar, G. N. *J. Am. Chem. Soc.* **1976**, *98*, 2804–2808.
(28) (a) Johnston, E.; Perrin, C. L. *J. Magn. Reson.*, **1979**, *33*, 619–626. (b) Faller, J. W. In "Determination of Organic Structures by Physical Methods"; Academic: New York, 1973; Vol. 5, pp 75–97.
(29) White, D. K.; Cannon, J.; Traylor, T. G. *J. Am. Chem. Soc.*, **1979**, *101*, 2443–2454.
(30) Farrar, T. C.; Becker, E. D. "Pulse and Fourier Transform NMR"; Academic: New York, 1971; pp 18–33.
(31) This result follows from the dependence of the saturation level on the T_1 and T_2 relaxation times: Pople, J. A.; Schneider, W. G.; Bernstein, H. J. "High Resolution Nuclear Magnetic Resonance"; McGraw-Hill: New York, 1959.
(32) Momenteau, M.; Rougee, M.; Loock, B. *Eur. J. Biochem.* **1976**, *71*, 63–76.
(33) Denniss, I. S.; Sanders, J. K. M. *Tetrahedron Lett.* **1978**, *3*, 295–298.
(34) Hoard, J. L. In "Porphyrins and Metalloporphyrins"; Smith, K., Ed.; Elsevier: New York, 1975; pp 359–368.
(35) (a) Berzinis, A.; Campbell, D.; White, D. K.; Traylor, T. G., manuscript in preparation. (b) We have shown that variations in this rotation angle greatly alter the contact shifts in cyanomet derivatives of chelated hemes, Berzinis, A.; Traylor, T. G. *J. Am. Chem. Soc.*, submitted.
(36) Geibel, J.; Cannon, J.; Campbell, D.; Traylor, T. G. *J. Am. Chem. Soc.* **1978**, *100*, 3575–3585.
(37) Brault, D.; Rougee, M. *Biochemistry* **1974**, *13*, 4591–4597.
(38) Satterlee, J. D.; La Mar, G. N.; Bold, T. J. *J. Am. Chem. Soc.* **1977**, *99*, 1088–1093, and references cited there.
(39) Rougee, M.; Brault, D. *Biochemistry* **1975**, *14*, 4100–4106.
(40) (a) Almog, J.; Baldwin, J. E.; Huff, J. *J. Am. Chem. Soc.* **1975**, *97*, 227–228. (b) Baldwin, J. E.; Klose, T.; Peters, M. *J. Chem. Soc., Chem. Commun.* **1976**, 881–883.
(41) Ogoshi, H.; Sugimoto, H.; Yoshida, Z. *Hukusokan Kogaku Torokai* **1975**, 239–243; *Chem. Abstr.* **1975**, *84*, 164069.
(42) Battersby, A. R.; Buckley, D. G.; Hartley, S. G.; Turnbull, M. D. *J. Chem. Soc., Chem. Commun.* **1976**, 879–881.
(43) Chang, C. K. *J. Am. Chem. Soc.* **1977**, *99*, 2819–2822.
(44) Collman, J. P.; Gagne, R. R.; Reed, C. A.; Halbert, T. R.; Lang, G.; Robinson, W. T. *J. Am. Chem. Soc.* **1975**, *97*, 1427–1439.
(45) Collman, J. P.; Reed, C. *J. Am. Chem. Soc.* **1973**, *95*, 2048–2049.
(46) Cannon, J.; Geibel, J.; Whipple, M.; Traylor, T. G. *J. Am. Chem. Soc.* **1976**, *98*, 3395–3396.
(47) Mincey, T.; Traylor, T. G. *Bioinorg. Chem.* **1978**, *9*, 409–420.
(48) (a) MacQuarrie, R.; Gibson, Q. H. *J. Biol. Chem.* **1971**, *246*, 5832–5835. (b) Sawicki, C. A.; Gibson, Q. H. *Ibid.* **1977**, *252*, 5783–5788.
(49) Brinigar, W. S.; Chang, C. K.; Geibel, J.; Traylor, T. G. *J. Am. Chem. Soc.* **1974**, *96*, 5597–5598.
(50) Weschler et al. report a similar trend in oxygen dissociation rates: Weschler, C. J.; Anderson, D. L.; Basolo, F. *J. Am. Chem. Soc.* **1975**, *97*, 6707–6713.
(51) (a) Maxwell, J. C.; Volpe, J. A.; Barlow, C. H.; Caughey, W. S. *Biochem. Biophys. Res. Commun.* **1974**, *58*, 166–171. (b) Maxwell, J. C.; Caughey, W. S. *Ibid.* **1974**, *60*, 1309–1314.
(52) Chang, C. K. *Appl. Spectrosc.* **1976**, *30*, 364–366.
(53) Schäfer, K.; Lax, E. "Landolt-Bornstein Tables"; Springer-Verlag: Berlin, 1962; Vol. 2, Part 2, pp 1–89.
(54) Gibson, Q. H. *Biochem. J.* **1959**, *71*, 293–296.
(55) Traylor, T. G. *J. Am. Chem. Soc.* **1963**, *85*, 2411–2413.
(56) Schwan, F. J. *J. Heterocycl. Chem.* **1967**, *4*, 633–634.
(57) Falk, J. E. "The Porphyrins and Metalloporphyrins"; Elsevier: New York, 1964; p 52.
(58) Wüthrich, K. *Struct. Bonding (Berlin)* **1970**, *8*, 73.

Enzyme Catalysis in Water Pools

F. M. Menger* and K. Yamada

Contribution from the Department of Chemistry, Emory University, Atlanta, Georgia 30322. *Received January 16, 1979*

Abstract: α-Chymotrypsin catalyzes the hydrolysis of *N*-acetyl-L-tryptophan methyl ester in water pools consisting of 0.11 M Aerosol OT and 2.8 M H_2O (buffered at pH 7.0 with 0.01 M phosphate) in heptane. The k_{cat} and K_M(app) were found to be 0.63 s^{-1} and 2.5×10^{-4} M (compared with 28 s^{-1} and 9.5×10^{-5} M for the same reaction in bulk water). Titration of the enzyme inside the pools with *p*-nitrophenyl acetate showed that the reduced activity at pH 7.0 is not the result of protein denaturation. Instead, the α-chymotrypsin solubilized in 95% heptane experiences a 1.5-unit shift to the right in its sigmoidal rate-pH profile. This shift places pH 7.0 on the low-pH plateau of the profile, thus greatly diminishing the apparent rate. At higher pH values (where the enzymatic rates reach their maximum), pool-incorporated enzyme actually has a *larger* k_{cat} than does enzyme in bulk water. Enzyme activity is insensitive to the pool size, which was varied from much smaller to much larger than the enzyme. This suggests that α-chymotrypsin molecules "create" their own micelles in the heptane rather than occupy empty ones already present. Circular dichroism studies indicate no major conformational changes in the protein within the water pools.

"Water pools" refer to inverted micelles containing a large quantity of water.[1-3] They are formed, for example, by adding water to heptane solutions of certain ionic surfactants such as bis(2-ethylhexyl)sodium sulfosuccinate (called Aerosol OT or AOT).[4-6] Presumably, clusters of water in the heptane are encased by AOT so that the alkyl chains lie in the aprotic solvent, whereas the sulfonate groups dip into the aqueous regions. A homogeneous mixture of 10% water in heptane can be prepared with only 0.1 M AOT.

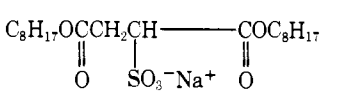

The recent discovery by Martinek, Berezin, and co-workers that enzymes dissolve and retain activity in water pools[7] prompts us to report now a detailed examination of α-chymotrypsin in water pool systems composed of 95–98% heptane. Apart from the inherent interest in determining how enzymes behave under these unusual conditions, we were motivated by the following questions: How does enzyme activity depend on the size of the water pools? What happens when the pool size becomes smaller than that of the enzyme? What is the pH-rate profile inside a pool? Does the enzyme experience pronounced conformational changes within the pool? How does substrate transport across the heptane-water boundary affect the enzyme kinetics? These questions concerning micellar chymotrypsin have not been previously addressed.

From a practical standpoint, pool-entrapped enzymes have potential utility in enzyme-mediated syntheses involving water-insoluble compounds. Incorporating enzymes into pools

0002-7863/79/1501-6731$01.00/0